Content Promotion for Online Content Platforms with the Diffusion Effect

Yunduan Lin[1], Mengxin Wang[2], Heng Zhang[3], Renyu Zhang[4], Zuo-Jun Max Shen[2]

[1] Civil and Environmental Engineering Department, University of California, Berkeley
[2] Industrial Engineering and Operations Research Department, University of California, Berkeley
[3] W. P. Carey School of Business, Arizona State University
[4] CUHK Business School, The Chinese University of Hong Kong

yunduan_lin@berkeley.edu,mengxin_wang@berkeley.edu,
hengzhang24@asu.edu,philipzhang@cuhk.edu.hk,maxshen@berkeley.edu

Problem Definition: Content promotion policies are crucial for online content platforms to improve content consumption and user engagement. However, traditional promotion policies generally neglect the diffusion effect within a crowd of users. In this paper, we study the candidate generation and promotion optimization (CGPO) problem for an online content platform, emphasizing the incorporation of the diffusion effect. **Methodology:** We propose a diffusion model that incorporates platform promotion decisions to characterize the adoption process of online content. Based on this diffusion model, we formulate the CGPO problem as a mixed-integer program with nonconvex and nonlinear constraints, which is proved to be NP-hard. Additionally, we investigate methods for estimating the diffusion model parameters using available online platform data and introduce novel double ordinary least squares (D-OLS) estimators. **Results:** We prove the submodularity of the objective function for the CGPO problem, which enables us to find an efficient $(1-1/e)$-approximation greedy solution. Furthermore, we demonstrate that the D-OLS estimators are consistent and have smaller asymptotic variances than traditional OLS estimators. By utilizing real data from a large-scale video-sharing platform, we show that our diffusion model effectively characterizes the adoption process of online content. Compared to the policy actually implemented on the platform, our proposed promotion policy increases total adoption by 49.90%. **Managerial Implications:** Our research highlights the essential role of diffusion in online content and provides actionable insights for online content platforms to optimize their content promotion policies by leveraging our diffusion model.

1. Introduction

In recent years, online content platforms such as Tiktok and Instagram have achieved considerable success in parallel with the proliferation of social media. These platforms offer various forms of online content, including reviews, blogs, and videos, with the content serving as virtual products to attract users. However, there are several unique features of online content platforms that set them apart from traditional online retailers. (i) *Platform objective*: While retailers aim to maximize the revenue obtained from selling products, content platforms aim to maximize the engagement of users and the impact of their content. For example, the total number of content clicks, which we adopt as the key metric in our work, is widely recognized as a vital metric for platform operations

(Su and Khoshgoftaar 2009) to measure content consumption. (ii) *Scale*: The amount of content is orders of magnitude larger than the number of products on an online retail platform. New content is generated at a significantly faster speed than new products introduced on an online retail platform. For instance, Amazon sells 12 million products in total (AMZScout 2021), while YouTube has more than 500 hours of videos (YouTube 2021) uploaded per minute, with an average video length of 11.7 minutes (Statista 2021). A rough estimate implies millions of new videos are uploaded every day. (iii) *User consumption behavior*: Unlike in an e-commerce setting where users directly search for a particular product of interest, online content platform users rely heavily on platform promotions and/or friends sharing content on a social network as ways to overcome information overload (Anandhan et al. 2018).

Therefore, online platforms actively promote content to users and foster an environment where users are encouraged to share interesting content. This leads to the phenomenon of content diffusion, wherein the content spreads to a larger audience beyond the scope of direct platform promotion. Consequently, a greater number of users have the opportunity to discover and consume the content, thereby significantly amplifying user engagement. Two examples of diffusion are provided below.

EXAMPLE 1 (THE DIFFUSION OF ONE PIECE OF CONTENT). Some articles that announce breaking news or tell good stories might go viral on the platform when many users cascadingly re-post them. For instance, in 2020, a local news story about two missing children in Florida netted almost 3.5 million shares on Facebook (FOX32 2020).

EXAMPLE 2 (THE DIFFUSION OF A TREND). Some content that is of the same category, similar in nature, or with homogeneous topics is usually associated with trending hashtags and/or headlines. As more users are aware of and engaged in this trend, the related content also becomes popular. For instance, the hashtag *#squidgame* has garnered 72.4 billion views on TikTok (TikTok 2021). Numerous TikTok users became part of the trend, and an enormous amount of content, including reenactments of the game, makeup looks, and Halloween costumes inspired by the TV show "Squid Game", was produced and viewed on TikTok.

The online content platform's business model prompts the following research question:

> *How can a promotion policy be designed that selects a small subset of content from the enormous corpus to display to users in a way that maximizes the total content clicks?*

The existing literature often prioritizes maximizing the number of clicks through direct promotion, while neglecting the diffusion effect. It advocates promoting content with a high historical click-through rate in hopes of attracting more direct clicks (Feng et al. 2007, Liu et al. 2010). However, this type of promotion may overemphasize already popular content, creating a scenario where a limited set of content is continuously promoted, reducing overall content diversity. This "rich get richer" phenomenon can negatively impact user engagement and satisfaction (Vahabi et al. 2015),

as users might be unable to discover new content. The challenge of the promotion policy lies in balancing between promoting trending content for immediate gain and promoting diverse content to stimulate user engagement for long-term platform sustainability. To the best of our knowledge, these trade-offs remain largely unexplored in the literature. The diffusion effect serves as one of the major sources of indirect gain. In this study, we aim to fill this gap by developing a diffusion-based promotion policy for online content platforms.

Machine learning-based promotion strategies in practice typically involve two stages: candidate generation and promotion optimization (Davidson et al. 2010, Covington et al. 2016). The candidate generation stage selects a small subset of content from a large corpus, while the promotion optimization stage allocates a limited promotion budget to each candidate content piece. This two-stage procedure balances computational efficiency and focuses the platform's attention on a small portion of content that can potentially generate high rewards. We follow this framework and introduce two distinct features that differ from previous machine learning-based strategies. First, we incorporate the diffusion effect into our promotion policy. Second, we recognize that the candidate set selection can impact the optimal allocation of user attention to the content. We therefore carefully consider these two stages together to maximize the total number of clicks, rather than treating them as separate machine learning tasks as in previous literature. This leads to the candidate generation and promotion optimization (CGPO) problem that we focus on in this paper.

A central piece of the CGPO problem is the promotion Bass diffusion model (P-BDM) that we propose to characterize the diffusion process of online content. The P-BDM is adapted from the well-known Bass diffusion model (BDM, Bass 1969) and inherits its innovative and imitative effects, which we interpret as two sources of user clicks on content platforms: platform promotion and diffusion through user sharing, respectively. We show that the BDM is not suitable for modeling the diffusion process of online content because it fails to account for platform promotion policy and the timeliness of content diffusion. In contrast, the P-BDM explicitly captures both and provides an excellent fit for a real-world online content platform. Based on the P-BDM, we offer a set of complete solution techniques for the online content promotion problem. Firstly, we integrate the candidate generation and promotion optimization problems into a succinct mixed-integer program, allowing us to obtain high-quality approximate solutions with performance guarantees. Secondly, leveraging the high-granularity data commonly available on online platforms, we design a novel estimation method for the parameters in the P-BDM. Lastly, our modeling framework, optimization algorithm, and estimation method are demonstrated to be effective through counterfactual analyses based on real online content data. In the next, we detail our contribution.

1.1. Contribution and Organization

- **A diffusion model for online content.** Our key contribution is the P-BDM for depicting online content diffusion, which takes into account the promotion policy and timeliness of content diffusion. Theoretically, the P-BDM characterizes the relationship between the platform's promotion decisions and the diffusion process, providing a concise way to optimize promotion policy. Practically, the P-BDM demonstrates effective alignment with real adoption patterns derived from an online video dataset.

- **Formulation and algorithmic design for the CGPO problem.** Under the P-BDM model, we represent the CGPO problem as a challenging mixed-integer optimization problem that involves complex dynamics of content adoption. Despite the presence of nonconvex and nonlinear constraints, as well as its proven NP-hardness, we identify a crucial property known as the "monotonic property with nested sets". This leads to the establishment of the submodularity of the problem objective. Leveraging this property, we propose the accelerated greedy algorithm (AGA), building upon the well-known greedy algorithm for submodular maximization problems (Nemhauser et al. 1978) with a $(1 - 1/e)$-approximation ratio.

- **New estimation approach for the P-BDM.** We introduce the double ordinary least squares (D-OLS) method for estimating P-BDM parameters, taking advantage of the online platform's ability to distinguish different types of adopters. D-OLS estimators are straightforward to compute and possess desired statistical properties. We show they yield smaller asymptotic variances compared to OLS estimators and demonstrate their robustness when the promotion policy is endogenous with diffusion dynamics theoretically and numerically.

- **Extensive numerical experiments with real data.** We validate our models and algorithms using a large-scale real-world data set from an online video-sharing platform. Our observations are threefold. First, the promotion and diffusion coefficients for online content are negatively correlated, highlighting the complexity of the CGPO problem. Second, the policy generated by the AGA effectively strikes a balance between incorporating the diffusion effect and updating the promotion policy. The success of the AGA provides invaluable insights, such as the emphasis on the promotion effect over the diffusion effect and the distinction of promotion strategies for various content based on their respective promotion and diffusion coefficients as well as content lifetime. Third, the AGA policy significantly outperforms the benchmark policy that disregards the diffusion effect, with an improvement of at least 49.90%.

The remainder of the paper is structured as follows: In Section 2, we review the related literature. In Section 3, we discuss the formulation of the P-BDM. In Section 4, we formulate the CGPO problem and propose the AGA for solving it. In Section 5, we discuss the estimation issues for the P-BDM and propose the D-OLS method. Section 6 presents our numerical studies based on real-world data, followed by concluding statements in Section 7.

2. Literature Review

As we discussed earlier, promotion and diffusion are two primary drivers of rewards for online content platforms. Therefore, we focus our review on promotion policies and diffusion effect studies. From the platform's perspective, its aim is to provide users with content that maximizes its total rewards. An active stream of literature is about recommender systems (RSs), which focuses on investigating the connections between users and content. Various recommendation algorithms (Kitts et al. 2000, Covington et al. 2016) have been proposed to evaluate the probability of users clicking on a particular item which characterizes the immediate interactions between the platform and users. Some recent work (Lu et al. 2014, Besbes et al. 2016) demonstrates that maximizing the immediate item relevancy does not align with utility maximization. The reasons are various, and one of the most important issues is the consequent diffusion within the social network. This implies that the adoptions are not only from directly targeted users but also from those who are influenced by them. Few studies incorporate this effect. Vahabi et al. (2015) are the first to mention that the social network can empower the utility maximization of RSs. They propose a social-diffusion-aware RS that can efficiently use recommendation slots and enhance the overall performance. Our work substantially differs from Vahabi et al. (2015). While they utilize a personalized recommendation scheme with a hard constraint that prevents neighbors from receiving identical content—we instead aim to characterize the diffusion trend across the population and find an optimal promotion policy.

We remark that our work does not emphasize understanding the relationship between users and content from a machine-learning perspective, as in the aforementioned literature. Typically, these works consider content recommendations for each user individually. Rather, we take a holistic approach and study the problem from an operations perspective. Our objective is to maximize the total clicks by modeling the whole problem as a diffusion process within the population and generating high-quality solutions using combinatorial optimization techniques.

To understand how user interactions influence adoptions, many diffusion models have been proposed in the marketing and information systems literature. Pioneered by Bass (1969), the BDM has become the most widely used model for new products, capturing the adoption trend with the use of parsimonious differential equations. A sequence of work (Easingwood et al. 1983, Norton and Bass 1987) extends the BDM by incorporating different dynamics, such as nonuniform influence and multiple generations. The BDM has achieved tremendous success in predicting the adoption of a variety of products, including consumer durable goods, medical innovations (Sultan et al. 1990), and information technology innovations (Teng et al. 2002). Despite its long history, the BDM continues to attract researcher attention and is frequently applied in novel contexts (Jiang and Jain 2012, Agrawal et al. 2021). Our diffusion model extends the BDM by integrating promotion policy

and the timeliness of online content diffusion. It follows the operations of online content platforms and explains the underlying diffusion behavior.

The BDM, along with all the other models previously referenced and our proposed model, focuses on the global diffusion effect. In particular, each user is influenced by a universal diffusion effect, namely the overall adoption level within the entire market. In contrast, some research has also explored diffusion in the context of social networks, where each user is influenced only by their local neighborhood. This type of diffusion model incorporates network structures and can provide a more granular representation of the unique diffusion effect experienced by each user. The independent cascade model (Goldenberg et al. 2001) and linear threshold model (Granovetter 1978) are two fundamental models that incorporate network structures. Kempe et al. (2003) then models the influence maximization problem as an algorithmic problem, aiming to identify the optimal subset of seed users that could trigger the maximum adoptions. For other applications, we refer readers to review papers (Kiesling et al. 2012, Zhang and Vorobeychik 2019). When considering the social network, researchers have found that diffusion can be impacted by the network structure (Manshadi et al. 2020), suggesting that an efficient targeting strategy should consider this structure (Eckles et al. 2022). However, the diffusion process within a network is not easy to quantify through a simple formula; hence, the market characterization relies heavily on simulation techniques, making the subsequent optimization problem time-consuming to solve. The challenge amplifies when attempting to devise a dynamic promotion policy with decisions changing over time, as considered in this work. Further, the network structure among users may not be observable or subject to change in reality, which increases the implementation difficulties. Given these limitations, our work focuses on the global diffusion effect to maintain simplicity and efficiency in optimization problems.

Another branch of study relevant to our work is revenue management for online retailers. While users exhibit different choice behaviors, the process of candidate selection and promotion optimization shares some similarities with assortment planning and pricing problems. Golrezaei et al. (2020) and Chen and Shi (2019) present the inventory and pricing strategies for strategic customers, who exhibit similar user behavior as online content platforms. Moreover, recent works also consider the network effect in operations management problems. Hu et al. (2016) consider the case where purchase decisions can be influenced by earlier purchases. Du et al. (2016), Wang and Wang (2017) propose a variant of the multinomial logit model incorporating the network effect in an assortment optimization problem. Follow-up works (Nosrat et al. 2021, Chen and Chen 2021) also involve different choice models. These studies utilize the problem structure of traditional assortment/pricing problems to achieve efficient algorithms. This line of research inspires us to consider similar problems on online content platforms.

3. Promotion Bass Diffusion Model

In this section, we introduce the promotion Bass diffusion model (P-BDM) to capture the adoption process of online content. We begin by highlighting a common issue of the Bass diffusion model to model the real-world online content adoption process. It motivates us to develop a new model, P-BDM, that incorporates the platform's promotion decisions, which serves as the foundation for our subsequent optimization and analysis.

3.1. Background and Motivation from a Large-Scale Video-Sharing Platform

We begin with a brief overview of the Bass diffusion model (BDM), which is a widely-used model for describing the adoption process of new products in a population over time. The basic premise of the BDM is that adopters can be classified into two types: *innovators* and *imitators*. Innovators are individuals who independently decide to adopt a product, while imitators are influenced by those who have already adopted it. In the context of online content, we view the clicks on a content piece as adoptions. For this reason, we use the terms "click" and "adoption" interchangeably throughout.

The discrete-time BDM models the adoption process of a product over a discrete finite time horizon $t = 1, 2, \ldots, T$ in a market of population size m. The initial number of adopters is denoted by A_0, and the number of new adopters at each time period t is given by:

$$a_t = \left(p + q\frac{A_{t-1}}{m}\right)(m - A_{t-1}), \quad \forall t = 1, \ldots, T, \tag{1}$$

where $A_{t-1} = A_0 + \sum_{\tau=1}^{t-1} a_\tau$ represents the cumulative number of adopters up to time period $t-1$, and p and q are the innovative and imitative coefficients, respectively. In particular, $(p + qA_{t-1}/m)$ corresponds to the adoption rate of the non-adopters at period t. This indicates that the adoption behavior at time t is jointly influenced by two forces: the innovative effect p and the imitative effect qA_{t-1}/m, which is proportional to the cumulative number of adopters. To ensure the discrete-time BDM is well-defined, it is commonly assumed that $p \geq 0$, $q \geq 0$, and $p + q \leq 1$.

Whereas it seems intuitive to apply the BDM to model the adoption of online content, empirical evidence may suggest otherwise. Particularly, we analyze the clickstream data from a large-scale video-sharing platform. For a detailed introduction about the platform and the data, please refer to Section 6.1. In Figure 1, we use a single video to showcase the typical pattern of the content diffusion process. In Figure 1(a), we present both the actual cumulative adoption data over 102 periods and the fitted BDM curve. The detailed explanation of our fitting method can be found in Section 5.1. Specifically, we first estimate the parameters of the BDM using data from the initial 60 periods, then use these parameters to generate a fitted curve for the full 102 periods. We evaluate the fitness and predictive power of this curve in two parts: from time period 0 to 60 and from 60 to 102. In the first part, although the fitted curve largely reflects the overall trend, it fails to capture
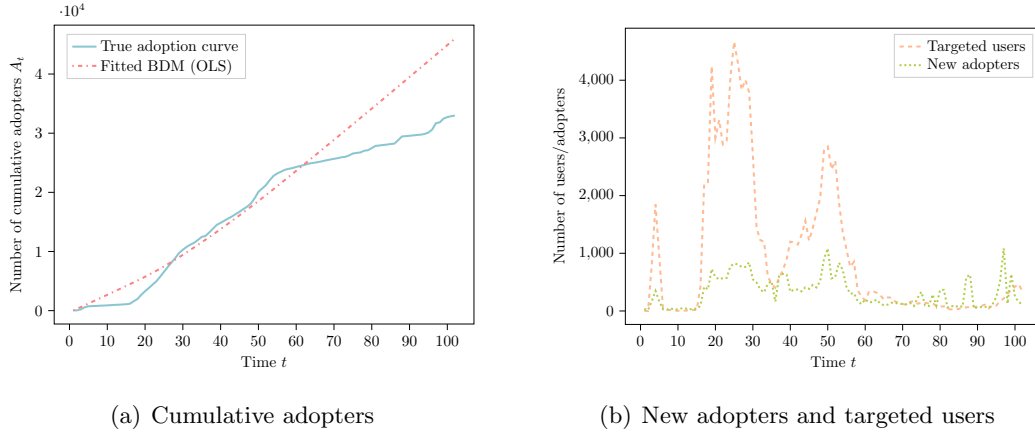
(a) Cumulative adopters

(b) New adopters and targeted users

Figure 1 **Illustration of adoption curves and the corresponding fitted BDM curve for an example video. (To ensure data anonymity, we have scaled the y-axis using a randomly selected number.)**

the subtle swings of the curve from time to time. In the second part, the fitted BDM continues to predict a steady growth of new adopters, whereas the actual data shows a much slower rate of adoption. As a result, the predicted adoption number deviates significantly from the actual value at the end. These observations suggest that the BDM may not be able to provide an appropriate description for the diffusion of online content. One of the significant factors contributing to this inconsistency is the BDM's assumption that all non-adopters will be impacted by the innovation effect, as outlined in Eqn. (1). However, this is unlikely to hold for online content due to limited user time and targeted promotion strategies. Figure 1(b) further supports this claim by showing a strong correlation between targeted users and new adopters at each time period.

The discrepancy between the BDM and actual adoption data is not unique to this particular example; it is commonly observed in the data. This suggests that platform-controlled promotion plays a vital role in driving adoption and motivates us to develop a new diffusion model tailored to online content that incorporates platform promotion policy.

3.2. The Promotion Bass Diffusion Model

The key message conveyed in the previous analysis is that one must take into account the platform's *promotion policy* to capture the adoption patterns of online content. This motivates our promotion Bass diffusion model (P-BDM). It builds on the notation of the BDM and adapts it to the specifics of online content. It aims to model the adoption process of online content over a finite time horizon $t = 1, 2, \ldots, T$ in a market of size m. The model posits that the adoption of a content piece is driven by two forces: (i) *promotion effect*, which reflects the intrinsic preference of users towards a content piece, specifically how likely a user is to adopt a content piece as an individual when it is promoted by the platform, and (ii) *diffusion effect*, which represents the influence of the adopted population on others, i.e., the likelihood that a user will adopt a content piece that is shared by other adopters.

The promotion and diffusion effects are the counterparts of innovative and imitative effects in the BDM; we, therefore, use these terms interchangeably in the following discussions. In a similar vein, we define the promotion coefficient p and diffusion coefficient q to characterize these two effects. Consistent with the BDM setting, we assume that $p \geq 0$, $q \geq 0$, and $p + q \leq 1$.

The P-BDM incorporates the platform's promotion policy as a new variable, denoted by $(x_t : t = 1, 2, \ldots, T)$, which represents the fraction of users in the market that receive the promotion at each time period. For mathematical convenience in the subsequent formulation, we define this promotion fraction over the entire market size rather than over the remaining non-adopters, although these two definitions can be converted to each other as needed. Specifically, there are in total mx_t users receiving the promotion at time t. To ensure that the platform does not promote the content piece to users who have already adopted it, the promotion fraction x_t is upper bounded by the fraction of the remaining non-adopters in the market at time $t-1$ (i.e., $x_t \leq 1 - A_{t-1}/m$). Denoting A_0 as the initial number of adopters, the P-BDM assumes that the number of new adopters at time t is

$$
a_t \;=\; \underbrace{\left(p + q\frac{A_{t-1}}{m}\right)mx_t}_{\text{Direct adopters}} + \underbrace{q\frac{A_{t-1}}{m}(m - A_{t-1} - mx_t)}_{\text{Indirect adopters}} \;=\; \underbrace{pmx_t}_{\text{Promotion effect}} \;+\; \underbrace{q\frac{A_{t-1}}{m}(m - A_{t-1})}_{\text{Diffusion effect}}. \quad (2)
$$

In the P-BDM dynamics (2), we categorize adopters based on whether they receive the promotion or not. For those not exposed to promotion, categorized as "indirect adopters", their adoption rate reflects only the diffusion effect and is expressed as qA_{t-1}/m. For those who receive the promotion, categorized as "direct adopters", their adoption rate is increased by the promotion effect, making it $(p + qA_{t-1}/m)$. It is worth noting that the BDM is a special case of the P-BDM where all non-adopters receive the promotion at each time period (i.e., $x_t = 1 - A_{t-1}/m, \forall t = 1, 2, \ldots, T$).

In practice, we also observe a *time decay effect* in online content diffusion, which can be attributed to the limited lifespan of content and the diminishing incentives for adopters to share it over time. To account for this timeliness feature, we incorporate a time-decay multiplicative factor γ for better alignment of the diffusion model with real-world data. We explain this approach in more detail in Section B.1.1. It is important to note that we consider the time-decay factor as an external influence, which means it does not complicate the theoretical analysis of the promotion optimization problem. Therefore, we assume $\gamma = 1$ until the discussion of numerical experiments (i.e., Section 6), where we will explore the effect of time-decay factor γ further.

4. Optimizing Content Adoptions

In practice, online platforms frequently undertake the mission of efficiently selecting and spotlighting featured content. This content, a distinct subset that the platform deliberately highlights or promotes, is usually selected due to its high quality and potential for stimulating trends. For

instance, on the platform with which we collaborate, algorithms select high-quality content regularly for inclusion in the "trending video pool". With the intent of stimulating diffusion and creating buzz, this content is then blended with other material—content selected based on user interests by machine learning algorithms, advertisements, and more—and displayed to users. The content display process on this platform is representative, including two stages (Davidson et al. 2010, Covington et al. 2016): candidate generation and promotion optimization. The former involves the selection of a promising subset of content from the overall corpus, while the latter necessitates the platform's allocation of its limited promotional resources among the selected candidates. This process, driven by machine learning and reliant on decentralized algorithms, doesn't account for overall diffusion—an objective of the trending video pool. In contrast, we formulate the content generation and promotion optimization (CGPO) problem as an optimization task to incorporate the diffusion effect into content promotion, using the P-BDM as a basis.

4.1. The Content Generation and Promotion Optimization Problem

We consider a platform with a fixed content corpus $\mathcal{V}$, operating within a market of unchanging size m. The platform can select up to K candidate content pieces. Its objective is to maximize total content adoptions over a fixed planning interval of length L given a promotion budget C. To achieve this, the platform needs to determine not only the promotion fraction for each content piece but also coordinate the timing of the promotion.

In line with the two-stage process, the platform first selects a subset $U \subseteq \mathcal{V}$ with no more than K candidates. This cardinality constraint reflects the natural upper bound on the size of the trending or featured video pool. Then, the platform determines the promotion policy $\boldsymbol{x} = (x_{v,t} : v \in U, t = 1, 2, \ldots, L)$ for the candidate set U. Here, each candidate $v \in U$ is promoted to a fraction $x_{v,t}$ of users at each time $t = 1, \ldots, L$. Subsequently, the CGPO problem is formulated as

$$\max_{U \subseteq \mathcal{V}:\ |U| \leq K} \quad R(U;C) + R(\mathcal{V} \setminus U; 0), \tag{3}$$

where $R(U;C)$ denotes the maximum total adoptions for the candidate set U, achievable by optimizing the promotion policy $\boldsymbol{x}$ within the promotion budget C. Similarly, $R(\mathcal{V} \setminus U; 0)$ denotes the total adoptions of the remaining set $\mathcal{V} \setminus U$ with budget 0. This is equivalent to none of the content pieces in the set $\mathcal{V} \setminus U$ being selected for promotion.

Notice that, function R can be depicted as the optimal value of an optimization problem. Given any $U \subseteq \mathcal{V}$ and promotion budget C, $R(U;C)$ is defined as the optimal value of the following promotion optimization (PO) subproblem:

$$\max_{\boldsymbol{x} \geq \boldsymbol{0}, \boldsymbol{A}_{U,1:L}} \quad \sum_{v \in U} A_{v,L} \tag{4a}$$

$$\text{s.t.} \qquad A_{v,t} = A_{v,t-1} + p_v m x_{v,t} + \frac{q_v}{m} A_{v,t-1}(m - A_{v,t-1}), \quad \forall v \in U \quad \forall t = 1,\ldots,L, \qquad (4b)$$

$$x_{v,t} \leq 1 - \frac{A_{v,t-1}}{m}, \qquad\qquad\qquad \forall v \in U \quad \forall t = 1,\ldots,L, \qquad (4c)$$

$$m \sum_{t=1}^{L} \sum_{v \in U} x_{v,t} \leq C. \qquad\qquad (4d)$$

In this subproblem, $\boldsymbol{A}_{v,:} = (A_{v,t} : t = 0, 1, \ldots, L)$ denotes the cumulative adopters for $v \in U$ at each time and initial adoption $\boldsymbol{A}_{v,0} = (A_{v,0} : v \in U)$ is given. The objective (4a) represents the total adoptions of all candidates in set U at the end of the L-period planning interval; (4b) mandates the cumulative adopters follow the P-BDM diffusion dynamics, as defined in Eqn. (2); (4c) ensures that the number of users receiving the promotion does not exceed the remaining non-adopters; (4d) ensures that across the L periods a total promotion budget C on the number of impressions can be used for promoting these videos in the featured video pool. The rest of platform capacity is reserved for other purposes such as displaying videos selected based on user interests and advertisements. In addition, we use $\bar{C} := C/mL$ to indicate the average promotion budget per user per time period, which can be an arbitrary given constant.

In a similar vein, we can define $R(\mathcal{V} \setminus U; 0)$. Specifically, it can be calculated according to the P-BDM diffusion dynamics (2) when $x_{v,t}$ is set to 0 for all $v \in \mathcal{V} \setminus U$ and $t = 1, 2, \ldots L$.

We remark on the following before solving the CGPO problem. First, on the notation side, we use bold notation to denote collections of specific variables for a set of content pieces within a certain time period, in vector or matrix form. For example, $\boldsymbol{x} = (x_{v,t} : v \in \mathcal{V}, t = 1, \ldots, L)$, $\boldsymbol{x}_{v,:} = (x_{v,t} : t = 1, \ldots, L)$, and $\boldsymbol{x}_{U,t} = (x_{v,t} : v \in U)$. We use $i : j$ to denote a slice of the vector or matrix ranging from index i to j, where $i, j \in \mathbb{Z}_+$. For example, $\boldsymbol{x}_{v,2:L} = (x_{v,t} : t = 2, \ldots, L)$. Second, one ultimate goal of content platforms is to maximize total adoptions over a long time horizon of T periods $(T \gg L)$. Crafting a "true" optimal promotion policy for this entire period is challenging due to the dynamic platform environment, including regular updates to the content corpus and market size variations. However, content diffusion on platforms typically outpaces these environmental changes (Graffius 2022). As such, it is reasonable to re-design promotion policies periodically for a short time period, in which the environment is relatively stable. The CGPO problem, therefore, seeks to identify such a dynamic policy within a L-period window. We can re-optimize it periodically to account for the environmental changes over the extended time horizon.

4.2. Promotion Optimization Given the Content Set

The CGPO problem inherently comprises two stages, namely, candidate generation (CG) and promotion optimization (PO). The CG stage, as represented in problem (3), is a combinatorial optimization problem that embeds the PO stage, as shown in problem (4). As proved in Section

A.1.1, the CGPO problem is NP-hard, making it challenging to solve. In this section, our focus is on the PO stage for a given candidate content set $U \subseteq \mathcal{V}$. We show how to optimally solve the PO subproblem and identify the key property that helps solve the CGPO problem.

Given the candidate set U, as a result of the P-BDM diffusion dynamics, the PO problem (4) remains difficult to solve due to its non-convex nature. In the following, we first perform convex relaxation and show that the PO problem is equivalent to its relaxed problem. Then, we highlight a critical ingredient in solving the relaxed problem, which is also an essential component of the algorithm used to address the entire CGPO problem.

4.2.1. Convex relaxation. The nonconvexity of problem (4) originates from the set of equality constraints (4b), which include a quadratic term of $\boldsymbol{A}$ in the right-hand side. To transform this nonconvex feasible region into a convex one, we relax (4b) as inequalities as follows:

$$A_{v,t} \leq A_{v,t-1} + p_v m x_{v,t} + \frac{q_v}{m} A_{v,t-1}(m - A_{v,t-1}), \quad \forall v \in U \ \ \forall t = 1, \ldots, L. \tag{5}$$

We denote the relaxed problem as PO-CR, which uses (4a) as the objective and includes (5), (4c), and (4d) as the constraints. The PO-CR problem is a convex optimization problem and thus can be handled by commercial solvers. Any optimal solutions to the PO-CR problem serve as upper-bound solutions to the PO problem (4). Moreover, as we illustrate in Theorem 1 below, the PO-CR problem is in fact equivalent to the original PO problem (4).

THEOREM 1 **(Relaxation).** *The PO problem* (4) *and relaxed problem PO-CR are equivalent.*

We remark that the equivalence is non-trivial because the decision variables $\boldsymbol{A}$ and $\boldsymbol{x}$ have opposing relationships in constraints (4b) and (4c). Specifically, increasing $A_{v,t}$ seems to increase the objective value due to (4b) but it lowers $x_{v,s}$ for $s \geq t+1$ due to (4c). To establish the equivalence, we need to show that the optimal solutions of the PO-CR problem are feasible solutions to the PO problem (4). The key intuition is that, under P-BDM dynamics, there is no benefit in "holding back" realized adoptions as a larger unadopted population for future promotion. In other words, achieving equality in constraint (4b) is more beneficial than maintaining the constraint as a strict inequality for a larger upper bound of $\boldsymbol{x}$ in constraint (4c). All missing proofs are in the appendix.

With the PO-CR problem at hand, we can directly find the optimal promotion policy for any given candidate set $U \subseteq \mathcal{V}$ using commercial solvers. However, to tackle the CGPO problem (3) as a whole, we need to utilize the optimality condition of the PO-CR problem, as detailed in Section 4.2.2, and then establish its link to the outer CG problem. This is accomplished by a reformulation that solely uses the promotion fraction $\boldsymbol{x}$ as the decision variable.

4.2.2.   Monotonic property with nested sets of PO problems. Given that the adoption number $\boldsymbol{A}_{v,1:L}$ intrinsically depends on $\boldsymbol{x}$ and $\boldsymbol{A}_{v,0}$, we logically reformulate the PO-CR problem into a convex program that solely involves the promotion fraction $\boldsymbol{x}$:

$$\max_{\boldsymbol{x}\geq\boldsymbol{0}}\quad \sum_{v\in U}f_v(\boldsymbol{x}_{v,:}) \tag{6a}$$

$$\text{s.t.}\quad m\sum_{t=1}^{L}\sum_{v\in U}x_{v,t}\leq C, \tag{6b}$$

$$x_{v,t}\leq 1-\frac{A_{v,0}}{m},\ \forall v\in U\ \ \forall t=1,\ldots,L, \tag{6c}$$

where for all $v\in U$, function $f_v(\boldsymbol{x}_{v,:})$ is defined as

$$f_v(\boldsymbol{x}_{v,:}):=\max_{\boldsymbol{A}_{v,1:L}}\quad A_{v,L}\quad\text{s.t.}\quad (5),(4c). \tag{7}$$

This reformulation utilizes a series of black-box functions, f_v for each $v\in U$, to evaluate the adoptions of content v under a given promotion policy. To ensure $f_v(\boldsymbol{x}_{v,:})$ is well-defined, we include a set of redundant constraints (6c) which ensures that problem (7) always has a feasible solution. We elaborate on the rationale behind these constraints and the process of constructing a feasible solution to problem (7) for any given policy in Section A.1.3. This reformulation creates a crucial link between the PO problem for a specific candidate set and the CG problem, which encompasses a set of PO problems for any possible candidate sets. It naturally divides the PO problem into two steps: evaluation and optimization. Evaluation is through functions f_v, separable for each content piece $v\in\mathcal{V}$ and independent of the chosen set U. For example, if we consider two different candidate sets U_1 and U_2 where $v\in\mathcal{V}$ is included in both sets, function f_v will be consistently defined across both PO problems. Moreover, the reformulation preserves the convexity of the PO-CR problem, as we can demonstrate that f_v is a concave function for each $v\in\mathcal{V}$ in Lemma 1.

LEMMA 1 **(Concavity).** *For any $v\in\mathcal{V}$, $f_v(\boldsymbol{x}_{v,:})$ is a concave function for $\boldsymbol{x}_{v,:}\in[0,1-A_{v,0}/m]^L$.*

Lemma 1 derives from the fact that problem (7) is a convex program. Based on this, we illustrate the optimality condition of the PO problem using the Lagrangian multiplier, which serves as a stepping stone to solving the entire CGPO problem. Specifically, we dualize the reformulation (6) as dual problem (8), with θ being the Lagrangian multiplier for constraint (6b):

$$\min_{\theta\geq 0}\quad \sum_{v\in U}h_v(\theta)+\theta C\,. \tag{8}$$

Here, $h_v(\theta)$ is defined as the optimal value function of the following maximization problem:

$$h_v(\theta):=\max_{\boldsymbol{x}_{v,:}\in[0,1-A_{v,0}/m]^L}f_v(\boldsymbol{x}_{v,:})-\theta m\sum_{t=1}^{L}x_{v,t}\,. \tag{9}$$

For any candidate set $U\subseteq\mathcal{V}$, let $\theta^*(U)$ denote the optimal dual variables of dual problem (8). In Lemma 2, we provide a comparison of optimal dual variables for nested candidate sets $U_1\subseteq U_2\subseteq\mathcal{V}$.

LEMMA 2 (**Monotonic property with nested sets**). *For any nested candidate sets $U_1 \subseteq U_2 \subseteq \mathcal{V}$, the optimal dual variables satisfy $\theta^*(U_1) \leq \theta^*(U_2)$.*

Lemma 2 implies that for two nested candidate sets, the optimal dual variables of the larger set will always be greater or equal. This conclusion is fundamentally grounded in the consistent definition of the function f_v across PO problems with different candidate sets. Lemma 2 not only enables us to efficiently search for the optimal dual solution θ^* without requiring a closed-form expression but also plays a crucial role in proving the submodularity of the outer GG problem in the subsequent section. In particular, we employ this monotonic property to show that the marginal gain of the CG problem decreases monotonically as the content set U enlarges.

4.3. Candidate Generation

In this section, we address the candidate generation (CG) stage, which aims to select a subset of content pieces that yield the maximum total adoptions. Leveraging the "monotonic property with nested sets" for PO problems derived in the previous section, we approach this combinatorial optimization from another perspective. Instead of directly identifying the optimal candidate set, we focus on the comparison of total adoptions between two nested candidate sets. By comparing the marginal gains of incorporating an additional content piece into nested candidate sets, we show that the objective of the CG problem (3) is a monotone submodular set function. This finding enables us to apply the greedy algorithm for submodular maximization to solve the entire CGPO problem, thereby achieving an $(1 - 1/e)$-approximation. Moreover, we can further accelerate the greedy algorithm by leveraging the "monotonic property with nested sets" again.

4.3.1. Submodularity of the CGPO objective. To verify that the CGPO objective (i.e., $R(U;C) + R(\mathcal{V} \setminus U; 0)$) is a submodular set function of $U \subseteq \mathcal{V}$, we need to show that $R(U \cup \{w\}; C) + R(\mathcal{V} \setminus (U \cup \{w\}); 0) - R(U; C) - R(\mathcal{V} \setminus U; 0)$ is decreasing in U, for all $w \in \mathcal{V} \setminus U$. With simple algebra, this is equivalent to showing that for any given nested sets $U_1 \subseteq U_2 \subseteq \mathcal{V}$ and $w \in \mathcal{V} \setminus U_2$,

$$R(U_1 \cup \{w\}; C) - R(U_1; C) - R(\{w\}; 0) \geq R(U_2 \cup \{w\}; C) - R(U_2; C) - R(\{w\}; 0). \quad (10)$$

The left and right sides of Eqn. (10) represent the marginal gain of adding an additional content piece w to sets U_1 and U_2, respectively. The marginal gain is characterized by the difference between the optimal values of two different PO problems. Direct comparison of two marginal gains is intractable, as the optimal value of PO problem does not have a closed-form expression. To overcome this challenge, in the following, we express the marginal gain as the difference between the optimal values of the same PO problem under different promotion budgets instead.

At a higher level, $R(U;C)$ denotes the optimal adoptions when the promotion budget C is entirely allocated to the candidate set U, whereas $R(U \cup \{w\}; C)$ denotes the optimal adoptions

when part of promotion budget $c \in [0, C]$ is allocated to U and the remaining $(C - c)$ is allocated to w. Hence, we can reformulate $R(U \cup \{w\})$ as the optimal value of the following problem:

$$R(U \cup \{w\}; C) := \max_{0 \leq c \leq C} [R(U; c) + R(\{w\}; C - c)], \tag{11}$$

where $R(U; c)$ is the maximum total adoptions of set U given a promotion budget c and $R(\{w\}; C - c)$ is the maximal total adoptions of content piece w with a promotion budget $(C - c)$.

Hence, if $c^*(U)$ denotes the optimal promotion budget allocated to set U in problem (11), the marginal gain from including content piece w given content set U can be expressed as

$$R(U \cup \{w\}; C) - R(U; C) - R(\{w\}; 0)$$
$$= [R(U; c^*(U)) - R(U; C)] + [R(\{w\}; C - c^*(U)) - R(\{w\}; 0)]. \tag{12}$$

As shown in Eqn. (12), the marginal gain is decomposed into two parts: the adoption loss of content set U due to the cannibalization of introducing the new content piece w, and the adoption gain resulting from w. Both parts can be depicted as the difference between optimal values of the same PO problem, with the promotion budget varied. This further enables us to use the Lagrangian multiplier to represent the marginal gain. Analogous to (8), we formulate the PO dual problem for content set U and promotion budget c as

$$R(U; c) = \min_{\theta \geq 0} \sum_{v \in U} h_v(\theta) + \theta c, \tag{13}$$

where $h_v(\theta)$ adheres to the same definition in Eqn. (9). By the envelope theorem, we can express the difference between two optimal values as an integral of the optimal dual variable, such as

$$R(U; c) - R(U; 0) = \int_{z=0}^{c} \theta^*(U; z) dz, \ \forall \ \theta^*(U; z) \in \Theta^*(U; z),$$

where $\Theta^*(U; z)$ is the set of optimal dual variables to problem (13) when the budget is z.

Consequently, the first term in Eqn. (12) can be represented as

$$R(U; c^*(U)) - R(U; C) = \int_{z=0}^{c^*(U)} \theta^*(U; z) dz - \int_{z=0}^{C} \theta^*(U; z) dz = -\int_{z=c^*(U)}^{C} \theta^*(U; z) dz.$$

In a similar manner, we can express the second term in Eqn. (12). Therefore, the marginal gain of adding piece w to the candidate set U can be represented by the optimal dual variables as

$$(12) = -\int_{z=c^*(U)}^{C} \theta^*(U; z) dz + \int_{z=0}^{C-c^*(U)} \theta^*(\{w\}; z) dz.$$

Hence, we transform the proof of submodularity, which essentially involves comparing the marginal gain of piece w over two nested sets U_1 and U_2, into a comparison between the optimal dual variables of PO problems with two nested sets. This leads us directly to Theorem 2.

THEOREM 2 **(Submodularity)**. *The CGPO objective, $R(U; C) + R(\mathcal{V} \setminus U; 0)$, is a monotone submodular set function with respect to content set $U \subseteq \mathcal{V}$.*

The proof of Theorem 2 relies on transforming marginal gain and utilizing the "monotonic property with nested sets". The complete proof is included in Section A.1.4. As a result, the CGPO problem (3) can be viewed as a monotone submodular maximization problem with a cardinality constraint.

4.3.2. Accelerated greedy algorithm. The well-known greedy algorithm (Nemhauser et al. 1978) provides an $(1 - 1/e)$-approximation for the monotone submodular maximization problem with a cardinality constraint. The algorithm iterates K times, selecting a content piece with the highest marginal gain in each iteration. The greedy algorithm is presented as Algorithm 1.

Algorithm 1: Greedy Algorithm for the CGPO Probem.

1 $U_0 := \emptyset$.

2 for $k \in [1, \ldots, K]$ **do**
3   **for** $v \in \mathcal{V} \setminus U_{k-1}$ **do**
4   Solve the PO problem (through its convex relaxation) for set $U_{k-1} \cup \{v\}$.
5   Let $R(U_{k-1} \cup \{v\}; C)$ be the optimal value.
6   **end**
7 $v^* := \arg\max_{w \in \mathcal{V} \setminus U_{k-1}} R(U_{k-1} \cup \{w\}; C) + R(\mathcal{V} \setminus (U_{k-1} \cup \{w\}); 0)$.
8 $U_k := U_{k-1} \cup \{v^*\}$.
9 end

Subsequently, we aim to demonstrate that an acceleration of the greedy algorithm can be achieved by exploiting the "monotonic property with nested sets". In each iteration, the greedy algorithm solves PO problems by adding an extra content piece to the previously selected set, which means it repeatedly solves PO problems for nested sets. Acceleration can be achieved by combining the Lagrangian relaxation technique with the greedy approach. The core idea is to utilize the optimal dual variable values from previously solved PO problems to create a more compact feasible region for subsequent iterations, which deals with expanded candidate sets. This approach results in a more efficient problem-solving process. We formalize this idea as the accelerated greedy algorithm (AGA), which is detailed as follows.

Accelerated Greedy Algorithm:

For Line 4 in Algorithm 1,

(i) At iteration k, record the optimal Lagrangian dual variable when solving the PO problem with set $U_{k-1} \cup \{v\}$ as $\theta^*(U_{k-1} \cup \{v\})$.

(ii) At iteration $k+1$, when solving the PO problem for set $U_k \cup \{v\}$, set the lower bound of Lagrangian dual variable as $\max\{\theta^*(U_k), \theta^*(U_{k-1} \cup \{v\})\}$.

As indicated by Lemma 2, the optimal dual variable monotonically increases with each greedy iteration. By implementing the AGA, we do not treat the PO problems as separate convex programming problems but rather utilize knowledge from previous iterations to speed up the solving process. In the AGA, the search region of the dual variable is adaptively shrunk at each greedy iteration by updating the lower bound to match the optimal dual variable from previous iterations. Consequently, the AGA can significantly reduce the execution time of optimizing the CGPO problem by exploiting the problem structure in conjunction with the greedy algorithm.

5.   Parameter Estimation

In this section, we discuss how to estimate the parameters of the P-BDM. We adapt the classical estimation methods for the BDM into our setting. We show that despite the challenges of estimating parameters for diffusion models, the high granularity of data available on online platforms allows us to achieve high-quality estimates, even when the promotion policy is endogenously determined throughout the diffusion process.

Although the BDM describes a deterministic diffusion dynamic, several probabilistic methods have been proposed to estimate its parameters. Bass (1969) first estimates the parameters using the ordinary least square (OLS) method. Schmittlein and Mahajan (1982), Srinivasan and Mason (1986) apply maximum likelihood estimation (MLE) and nonlinear least square to obtain better estimates. However, these methods and their analysis are complicated by the diffusion nature, such as autocorrelation, which exists among observations because diffusion happens as a dynamic process. The new adoptions at each time step depend on the previous cumulative adoption number and affect future adoptions. The intricate relationship of parameters, such as the cumulative adopters as a direct function of p, q, and m, further complicates the problem (a commonly used expression can be founded in Schmittlein and Mahajan 1982). These issues degrade the performance of the estimators. Estimating the parameters of the P-BDM introduces additional challenges due to promotion activities, beyond the issues already present in the BDM. The inclusion of promotion decisions makes the closed-form expression of cumulative adopters no longer exist, limiting our choice of estimation tools. Additionally, as we discussed in this work, the platform usually determines promotion policy based on real-time market adoption levels, making the promotion fraction correlated with the cumulative adopters and thus endogenous in the diffusion dynamics.

We revisit the OLS and MLE methods for the BDM and adapt them to the P-BDM, leading to new estimation methods, namely the D-OLS and D-MLE methods. We highlight that, while there are inherent deficiencies in estimating diffusion models as mentioned above, we can largely

alleviate these issues and improve the estimation results on online platforms. In fact, compared to traditional markets, we can extract additional information from online platforms, particularly by identifying adopters who have received promotions. We use a fixed design framework to underscore the theoretical benefits of this extra information. Although this analysis is stylized, the benefits we demonstrate are not merely fortuitous; they are also consistently observed in numerical experiments with both OLS-based and MLE-based estimators.

In the following discussions, we focus on a fixed $v \in \mathcal{V}$ and omit the subscript v and treat the market size m as fixed.

5.1. OLS Estimators

In this part, we discuss the OLS-based methods for estimating parameters in the P-BDM. We base our approach on the OLS method for the BDM as presented in Bass (1969), summarized in Section A.2.1. To estimate parameters in the P-BDM, we observe a sequence of observations $\{(a_t, x_t, A_t)\}_{t=1}^{T}$, which includes both the realization of promotion decisions and adoption numbers. The OLS method for the P-BDM relies on the following relationship:

$$a_t = p \cdot mx_t + q \cdot \frac{A_{t-1}}{m}(m - A_{t-1}) + \epsilon_t \,,$$

where p and q are the two parameters to estimate and ϵ_t is independent random noise with mean 0, as defined in the OLS estimation for the BDM. We obtain OLS estimators for p and q by considering mx_t and $(A_{t-1} - A_{t-1}^2/m)$ as two observed covariates. However, since the promotion fraction often correlates with adoption numbers, there can be certain colinearity between these two covariates, resulting in OLS estimators possibly yielding large variances. Note that when $x_t = 1$ for all t, this is the classical OLS method for the BDM.

To reduce the variances, we can leverage information about adopter types on online platforms. Specifically, out of the total new adopters (a_t), we can observe the number of direct adopters who receive the promotion (a_t^{d}) and the number of indirect adopters who do not receive the promotion (a_t^{i}). This yields a sequence of adoption data $\left\{(a_t^{\mathrm{d}}, a_t^{\mathrm{i}}, A_t, x_t)\right\}_{t=1}^{T}$. We propose a straightforward double-OLS (D-OLS) method based on the following relationships:

$$a_t^{\mathrm{d}} = p \cdot mx_t + q \cdot A_{t-1}x_t + \epsilon_t^{\mathrm{d}} \quad \text{and} \quad a_t^{\mathrm{i}} = q \cdot \frac{A_{t-1}}{m}(m - A_{t-1} - mx_t) + \epsilon_t^{\mathrm{i}}, \tag{14}$$

where the first equation in (14) focuses on the direct adopters targeted by promotion while the second focuses on the others; ϵ_t^{d} and ϵ_t^{i} are independent random noises such that $\epsilon_t = \epsilon_t^{\mathrm{d}} + \epsilon_t^{\mathrm{i}}$.

Our D-OLS method yields estimators, $\hat{p}^{\mathrm{D\text{-}OLS}}$ and $\hat{q}^{\mathrm{D\text{-}OLS}}$, through the following steps:

(i) We use the OLS method to estimate $\hat{q}^{\mathrm{D\text{-}OLS}}$ from the second equation in (14), resulting in:

$$\hat{q}^{\mathrm{D\text{-}OLS}} = \frac{\sum_{t=1}^{T}\left[A_{t-1}(1 - x_t - \frac{A_{t-1}}{m})a_t^{\mathrm{i}}\right]}{\sum_{t=1}^{T}\left[A_{t-1}(1 - x_t - \frac{A_{t-1}}{m})\right]^2}\,;$$

(ii) We use the OLS method again, but this time we substitute q in the first equation in (14) with the D-OLS estimator $\hat{q}^{\text{D-OLS}}$, to compute $\hat{p}^{\text{D-OLS}}$, which is given by:

$$\hat{p}^{\text{D-OLS}} = \frac{\sum_{t=1}^{T} \left[m x_t (a_t^{\text{d}} - \hat{q}^{\text{D-OLS}} A_{t-1} x_t) \right]}{\sum_{t=1}^{T} (m x_t)^2}.$$

By separating the estimation of two coefficients, the D-OLS method also alleviates the issue of correlation between the promotion fraction and adoption number. This method reduces the variance of estimators and enhances prediction accuracy. In the next section, we illustrate this improvement by analyzing the asymptotic properties of these estimators.

5.1.1. Asymptotic properties. We now examine the asymptotic properties of the estimators. Our analysis reveals that D-OLS estimators are $\sqrt{n}$-consistent and possess smaller asymptotic variances than OLS estimators. Moreover, the reduction in variance becomes more pronounced when the promotion policy is endogenous with the diffusion dynamics.

In the traditional BDM literature, rigorous asymptotic analysis of estimation has been a challenging task due to the lack of an asymptotic framework for diffusion processes. To flesh out the comparison between OLS and D-OLS estimators, we consider a fixed design framework with a triangular sequence of infinite diffusion processes. Specifically, we consider a sequence of diffusion processes with an increasing market size $m_{(n)}$ for $n = 1, 2, \ldots$. We assume the observations come from a fixed-design triangular array, wherein the n-th row includes n observations from the diffusion process with market size $m_{(n)}$. We treat the covariates as fixed rather than random variables. This creates a framework amenable to theoretical analysis. For the n-th diffusion process, let $\left\{ A_{i,(n)} \right\}_{i=1}^{n}$ denote the adopters at n different time steps and $\left\{ x_{i,(n)} \right\}_{i=1}^{n}$ denote the consequent promotion fractions. We then define the empirical second-moment matrices of the OLS method, as well as the empirical second moments of the two estimation steps in the D-OLS method as follows:

$$Q_{(n)} = \begin{pmatrix} \frac{1}{n} \sum_{i=1}^{n} x_{i,(n)}^2 & \frac{1}{n} \sum_{i=1}^{n} x_{i,(n)} \bar{A}_{i,(n)} (1 - \bar{A}_{i,(n)}) \\ \frac{1}{n} \sum_{i=1}^{n} x_{i,(n)} \bar{A}_{i,(n)} (1 - \bar{A}_{i,(n)}) & \frac{1}{n} \sum_{i=1}^{n} \left[\bar{A}_{i,(n)} (1 - \bar{A}_{i,(n)}) \right]^2 \end{pmatrix},$$

$$\tilde{Q}_{11,(n)} = \frac{1}{n} \sum_{i=1}^{n} x_{i,(n)}^2 \bar{A}_{i,(n)}, \text{ and } \tilde{Q}_{22,(n)} = \frac{1}{n} \sum_{i=1}^{n} \bar{A}_{i,(n)}^2 (1 - x_{i,(n)} - \bar{A}_{i,(n)})^2.$$

where $\bar{A}_{i,(n)} = A_{i,(n)} / m_{(n)}$ is the normalized adopter number (i.e., the fraction of adopters).

Our analysis is based on the following assumption, common for regression in fixed-design settings and reasonable in practice. With Q defined in the assumption, we let Q_{11} be the component in row one and column one of Q. Other components can be defined in a similar fashion.

ASSUMPTION 1 (**Positive Definiteness**). *We assume that the following limits exist:*

$$\lim_{n \to \infty} Q_{(n)} = Q, \ \lim_{n \to \infty} \tilde{Q}_{11,(n)} = \tilde{Q}_{11}, \ \text{and} \ \lim_{n \to \infty} \tilde{Q}_{22,(n)} = \tilde{Q}_{22},$$

where Q is positive definite and $\tilde{Q}_{11}, \tilde{Q}_{22} > 0$.

We further suppose the scaled random noise for the n-th diffusion process $\bar{\epsilon} := \epsilon/m_{(n)}$ has variance σ^2. The following theorems, Theorem 3 and Theorem 4, show the asymptotic properties of D-OLS estimators. The detailed proof is given in Section A.2.2.

THEOREM 3 (**Consistency**). *Suppose that the scaled random noise* $\bar{\epsilon}_i^i := \epsilon_i^i/m_{(n)}$ *and* $\bar{\epsilon}_i^d :=$ $\epsilon_i^d/m_{(n)}$ *are independently and identically distributed with mean zero and finite variance for all* $i = 1, \dots, n$, *then D-OLS estimators* $\hat{p}^{D\text{-}OLS}$ *and* $\hat{q}^{D\text{-}OLS}$ *converge to the true parameters* p *and* q *in probability as* n *scales to infinity. That is,*

$$\hat{p}_{(n)}^{D\text{-}OLS} \xrightarrow{p} p \text{ and } \hat{q}_{(n)}^{D\text{-}OLS} \xrightarrow{p} q.$$

Theorem 3 implies that with sufficient observations, the true values of p and q can be uncovered.

THEOREM 4 (**Asymptotic Normality**). *Suppose that the scaled random noise* $\bar{\epsilon}_i^i$ *and* $\bar{\epsilon}_i^d$ *are independently and identically distributed with mean zero and variance* $(1-\eta)\sigma^2$ *and* $\eta\sigma^2$ *for all* $i = 1, \dots, n$ *for some* $\eta \in (0,1)$, *then when* n *scales to infinity,*

(i) *D-OLS estimators* $\hat{p}_{(n)}^{D\text{-}OLS}$ *and* $\hat{q}_{(n)}^{D\text{-}OLS}$ *are asymptotically normal. Specifically,*

$$\sqrt{n}\left(\hat{p}_{(n)}^{D\text{-}OLS} - p\right) \xrightarrow{d} \mathcal{N}\left(0, \frac{1}{Q_{11}}(1+\xi_1)\sigma^2\right) \text{ and } \sqrt{n}\left(\hat{q}_{(n)}^{D\text{-}OLS} - q\right) \xrightarrow{d} \mathcal{N}\left(0, \frac{1}{Q_{22}}(1+\xi_2)\sigma^2\right),$$

where $\xi_1 = \eta(\tilde{Q}_{11}^2/\tilde{Q}_{22}Q_{11} - 1)$ *and* $\xi_2 = \eta Q_{22}/\tilde{Q}_{22} - 1$.

(ii) *OLS estimators* $\hat{p}_{(n)}^{OLS}$ *and* $\hat{q}_{(n)}^{OLS}$ *are asymptotically normal. Specifically,*

$$\sqrt{n}\left(\hat{p}_{(n)}^{OLS} - p\right) \xrightarrow{d} \mathcal{N}\left(0, \frac{1}{Q_{11}}(1+\kappa)\sigma^2\right) \text{ and } \sqrt{n}\left(\hat{q}_{(n)}^{OLS} - q\right) \xrightarrow{d} \mathcal{N}\left(0, \frac{1}{Q_{22}}(1+\kappa)\sigma^2\right),$$

where $\kappa = Q_{12}^2/|Q|$.

We draw two insights based on Theorem 4. First, the ratio κ is not negligible, especially when the promotion policy is endogenous with diffusion dynamics. We observe that κ increases as the determinant of Q decreases. When x is highly colinear to $\bar{A}(1 - \bar{A})$, κ approaches infinity while ξ_1 and ξ_2 remain bounded. Therefore, D-OLS estimators are more robust against correlations than OLS estimators. Second, when $\eta \le \tilde{Q}_{22}/Q_{22}$, D-OLS estimators have smaller asymptotic variances than OLS estimators (see Proposition 1, Section A.2). We note that, according to our real-world data set, the average of promotion fraction x_t is 0.00062 per hour, placing $\tilde{Q}_{22}/Q_{22}$ in close proximity to one. Consequently, we expect $\eta \le \tilde{Q}_{22}/Q_{22}$ to be readily fulfilled in our setting, suggesting that D-OLS estimators present smaller asymptotic variances than OLS estimators. The advantage of D-OLS is clearly observed in subsequent numerical experiments.

5.2. MLE Estimators

While the OLS method is straightforward and computationally efficient, it lacks a rigorous probabilistic interpretation in a diffusion setting. On the other hand, the MLE method in Schmittlein and Mahajan (1982) for estimating the BDM is based on a rigorous probabilistic model. However, it requires an explicit expression of the cumulative adopter number A_t, which is not applicable in the P-BDM. Nonetheless, we show that MLE-based estimators can still be used in our setting.

When the platform cannot distinguish different adopter types, the probabilistic counterpart is established as follows: At time t, there are $(m - A_{t-1})$ non-adopters, each of which has the same adoption probability as $(px_t/(1 - A_{t-1}/m) + qA_{t-1}/m)$. The log-likelihood function is formulated as

$$\mathcal{LL}^{\mathrm{MLE}}(p,q) = \sum_{t=1}^{T} a_t \log\left(\frac{mx_t}{m - A_{t-1}}p + \frac{A_{t-1}}{m}q\right) + (m - A_{t-1} - a_t)\log\left(1 - \frac{mx_t}{m - A_{t-1}}p - \frac{A_{t-1}}{m}q\right).$$

When the platform can distinguish adopter types, the probabilistic counterpart is established as follows: At time t, there are $(m - A_{t-1})$ non-adopters. Each non-adopter has a probability of $mx_t/(m - A_{t-1})$ to be promoted by the platform. Given being promoted, the non-adopters adopt independently with probability $(p + qA_{t-1}/m)$. Otherwise, the non-adopters adopt independently with probability qA_{t-1}/m when not being promoted. The log-likelihood function is formulated as

$$\mathcal{LL}^{\mathrm{D\text{-}MLE}}(p,q) = \sum_{t=1}^{T}\left[a_t^{\mathrm{i}}\log\left(\frac{A_{t-1}}{m}q\right) + (m - A_{t-1} - mx_t - a_t^{\mathrm{i}})\log\left(1 - \frac{A_{t-1}}{m}q\right)\right]$$
$$+ \sum_{t=1}^{T}\left[a_t^{\mathrm{d}}\log\left(p + \frac{A_{t-1}}{m}q\right) + (mx_t - a_t^{\mathrm{d}})\log\left(1 - p - \frac{A_{t-1}}{m}q\right)\right],$$

and the derived estimators are named D-MLE estimators. In Section A.2.3, we show that both log-likelihood functions are concave, allowing us to use the gradient method for estimation.

5.3. Comparing OLS-Based and MLE-Based Estimators with Simulation

We create a synthetic dataset by bootstrapping the diffusion processes of a content piece according to P-BDM dynamics. The diffusion processes are simulated based on the D-MLE probabilistic counterpart defined in Section 5.2 when adopter types can be distinguished. We assess the estimators under two promotion schemes: (i) Const: promotion fraction x_t remains constant; (ii) Linear: promotion fraction x_t has a positive linear relationship with adopter number A_{t-1}.

The true values of coefficients are set at $p = 0.523$ and $q = 0.062$. We run experiments with market sizes ranging from $m = 1,200$ to $m = 40,000$, and scale observation numbers with market size, as mentioned in Section 5.1.1. Performance is measured using estimation error of the parameters, which is the Euclidean distance between the estimators and true values $\sqrt{(p - \hat{p})^2 + (q - \hat{q})^2}$.
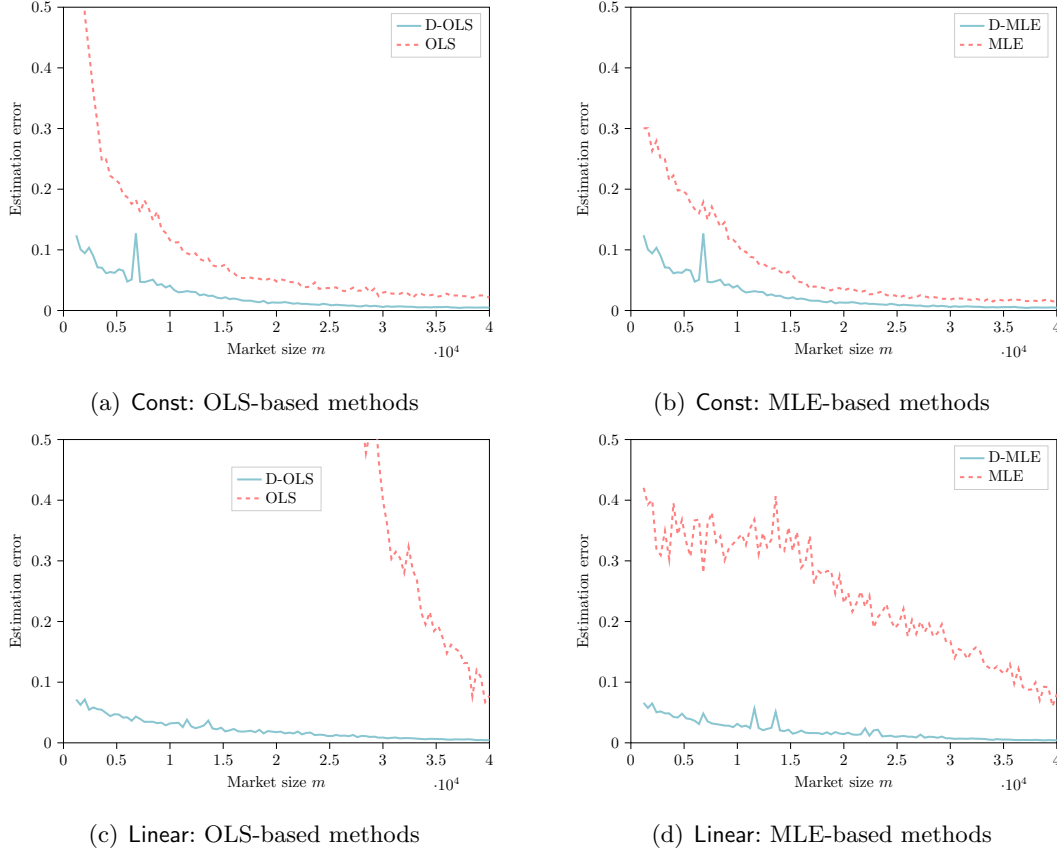
(a) Const: OLS-based methods

(b) Const: MLE-based methods

(c) Linear: OLS-based methods

(d) Linear: MLE-based methods

Figure 2   **Estimation errors for different methods against market size (scale with the number of observations).**

Figure 2 displays the results for Const and Linear schemes, respectively. Overall, we observe a significant improvement when adopter types can be distinguished, emphasizing the benefits of using additional data for estimating diffusion models. We offer two more observations. First, comparing Figures 2(a) with 2(c), and Figures 2(b) with 2(d), we see larger relative improvements under the Linear scheme compared to the Const scheme, particularly for OLS-based estimators. This not only indicates robustness in MLE-based methods but also verifies the theoretical results in Theorem 4 and highlights the effectiveness of our proposed estimators in real-world online platforms, where the promotion policy is typically endogenous. Second, comparing Figures 2(a) and 2(b), or Figures 2(c) and 2(d), we notice that D-OLS and D-MLE perform similarly when adopter types can be distinguished, while the MLE method outperforms the OLS method when they cannot be differentiated. In this case, the correlation among covariates creates difficulty for OLS estimators, but additional information about adoption types helps to greatly narrow the gap.

In summary, both the D-OLS and D-MLE methods perform well when working with data available on online platforms. While the D-MLE method is supported by a rigorous probabilistic framework, it is less computationally efficient. Given the similar performance of D-OLS and D-MLE, we opt to use the D-OLS method for other computational experiments with real data.

6. Numerical Results

In this section, we conduct a comprehensive counterfactual analysis using a real-world data set from a large-scale video-sharing platform. At a high level, we test the performance of the AGA promotion policy with this data set.

6.1. Platform and Data Overview

We obtain the data set from one of the most popular Chinese video-sharing platforms, similar to TikTok. The platform is fueled by user-generated content and has become a social phenomenon, with a massive user base sharing their daily lives. As of 2023, it has over 360 million daily active users and over 20 billion videos. Effective content promotion plays an important role in platform operations. While machine learning-based algorithms offer personalized recommendations curated based on user interests, promoting content that has the potential to go viral is challenging due to the difficulty of optimizing diffusion. As such, the issue addressed in this study is essential for the platform to maximize its impact and foster an engaged user community.

The data set consists of user behavior logs for 46,444 short videos, sampled from 518,646 users over 20 days (7/1/2020-7/20/2020). The logs contain timestamped records of video promotions and user behavior in terms of clicks. For each video, we identify two distinct user sets: $\mathcal{L}_P$, which comprises users who receive the promotion, and $\mathcal{L}_C$, which comprises users who click on it. It should be noted that due to the presence of diffusion effects, some users click on videos without receiving promotions (i.e., $\mathcal{L}_C \setminus \mathcal{L}_P \neq \emptyset$).

For ease of analysis, we aggregate the timestamped data hourly. In each hour, we calculate the promotion fraction as the ratio between the promoted users ($\mathcal{L}_P$) and market size m. We further identify adopter types: direct adopters ($\mathcal{L}_P \cap \mathcal{L}_C$) and indirect adopters ($\mathcal{L}_C \setminus \mathcal{L}_P$). In addition, each video is categorized by the platform according to its topic, such as travel, education, game, etc. This information is provided to us while ensuring anonymity. The dataset includes videos from 61 category labels provided by the platform, ranging from 155 to 2,759 videos per category.

6.2. Model Calibration

In this section, we estimate the promotion and diffusion coefficients under the P-BDM specification with the real-world video data, comparing results with the BDM benchmark.

We use the D-OLS method to estimate p and q. During this process, we consider the following two key aspects. (i) *Time-decay factor*: We include a time-decay factor γ as a hyperparameter to reflect users' decreasing tendency to share content over time. See Section B.1.1 for more details. (ii) *Group estimation*: We estimate the same p and q values for each video category. We highlight that often times promotion decisions are made at the early stage of a video's life cycle with minimal data available for estimation. Consequently, group-wise estimation is typically utilized to guarantee

generalizability and precision. For the sake of simplicity in this study, we use the category labels provided by the platform to determine groups. See Section B.1.2 for more details. For more about our calibration process, including data splitting, hyperparameter selection, and the effect of time-decay factor γ on results, please refer to Section B.1.3. Next, we present the calibration results under the best time-decay factor $\gamma = 0.983$.

Distribution of p and q: Figure 3 depicts the distribution of estimated coefficients across 61 different categories. The promotion coefficient p ranges from 0.028 to 0.325, and the diffusion
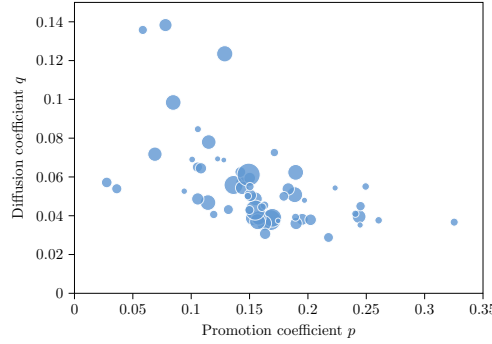

Figure 3   **Distribution of estimated promotion coefficient p and diffusion coefficient q. Each point in the scatter plot represents a video category. The size of points represents the number of videos in each category.**

coefficient q ranges from 0.029 to 0.138. Notably, a negative correlation between p and q is observed, with a Pearson correlation coefficient of $\rho = -0.5335$. A one-tailed t-test further supports the negative correlation, with a t-statistic of -4.845 rejecting the null hypothesis at a significance level of 0.05 (critical t-value of -1.671). These findings suggest that videos attracting users via promotion may not necessarily have a larger diffusion effect, highlighting the complexity of the CGPO problem and the need for a promotion policy that accounts for the diffusion effect.

Performance of estimation: We evaluate the performance using the weighted mean absolute percent error (WMAPE), which can be calculated as $\text{WMAPE} = \sum_{t=1}^{T_v} |a_{v,t} - \hat{a}_{v,t}| / \sum_{t=1}^{T_v} a_{v,t}$ for video v, where $\hat{a}_{v,t}$ is the predicted number for new adopters. Overall, the P-BDM estimated with the D-OLS method achieves an average out-of-sample WMAPE of 38.96%. We assess the D-OLS approach with the P-BDM against two benchmarks. Our first point of comparison is the traditional OLS method, an examination that underscores the advantages of the D-OLS method in the context of online platforms. Secondly, we contrast the P-BDM with the BDM, demonstrating the P-BDM's superior aptitude in managing online content adoptions. The out-of-sample WMAPEs for these two benchmarks register at 39.66% and 81.25% respectively. The P-BDM shows a considerable improvement over the BDM and a moderate yet noticeable enhancement compared to the OLS method. In contrast to the simulation in Section 5.3, the colinearity issue brought up in Section 5.1.1

is not severe in this dataset. This explains the reason for the scale of this latter difference. Through the use of a paired t-test, we ascertain that the improvement, while smaller in scale, is statistically significant with a t-statistic of -35.48, significantly smaller than the t-value corresponding to a 0.05 significance level (i.e., -1.645). Further, when we perform hypothesis tests for each category, we find that 53 out of the 61 categories display improvement at the 0.05 significance level. Two categories indicate deterioration, while the remaining six categories do not show significant changes.

To further illustrate the effectiveness of the P-BDM in capturing online content adoption, we present two examples in Figure 4. The left subfigure 4(a) uses the same video as the motivating example in Section 3.1. To clearly delineate the issue, we estimate the coefficients from a single video, rather than the entire category. That is, for each video, we use the first 60% data samples to estimate coefficients and generate the fitted curves for the entire time horizon using the estimated coefficients. Compared to the BDM, the P-BDM fits not only the overall adoption trend but also
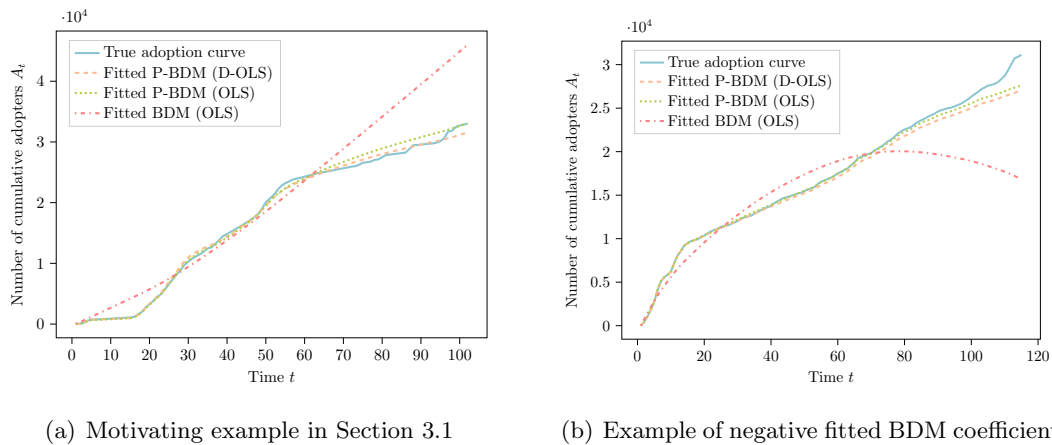

(a) Motivating example in Section 3.1   (b) Example of negative fitted BDM coefficient

Figure 4   **Illustration of adoption curves and the corresponding fitted BDM/P-BDM curves for example videos. (To ensure data anonymity, we have scaled the y-axis using a randomly selected number.)**

the curve shape, especially in the early time periods. Subfigure 4(b) further shows another typical scenario, for which the estimated BDM coefficients are negative. We can still see a good fit in early periods, but in general, this result lacks a valid real-world interpretation. These examples highlight the importance of using the P-BDM to accurately capture online content adoption.

6.3. Experiments on the Accelerated Greedy Algorithm

In this section, we simulate an online platform environment with previously estimated parameters to evaluate different promotion policies. We name the promotion policy recommended by the AGA under the P-BDM as the AGA policy.

6.3.1. Long-term performance with different planning intervals. In practice, platforms are concerned with the long-term efficacy of promotion policies. Accordingly, we solve the CGPO problem every L periods using the AGA policy in the most recent platform environment.

We run the simulation over a 120-period time horizon with a market size of $m = 10,000$. The platform can promote from a candidate set with a capacity of $K = 50$. We assess the AGA policy by varying the planning interval L from 1 to 20 and the average promotion budget per user per period $\bar{C}$ from 2 to 10. More details are described as follows.

- *Video corpus*: The video corpus is initialized at $t = 0$ with 50 videos, all with zero adoptions. We assume that at each time step, 5 new videos are added with no initial adoptions, to be consistent with the practical operations of the platform. Each video is associated with parameters (p, q) randomly sampled from the empirical distribution estimated in Section 6.2.
- *User behavior*: At each time, users act according to the D-MLE stochastic counterpart of the P-BDM, as described in Section 5.2.
- *AGA implementation.* We assume that the platform employs the AGA with a planning interval of L. We solve the CGPO problem every L periods and implement the policy recommended by the AGA for these L periods. To keep the policy up-to-date with the platform environment, new videos added during the past L periods are included when solving the new CGPO problem instance, with initial adoption numbers set to match those at the end of the past L periods.

We first remark that the selection of L is crucial in striking the balance between the frequency of policy updates and the consideration of diffusion effects. A smaller L permits more frequent policy updates yet is myopic and ignores diffusion in the long term. Conversely, a larger L considers more extended diffusion effects but may delay the promotion of new videos due to less frequent policy updates. When $L = 1$, the AGA policy is equivalent to ignoring all diffusion effects. This tradeoff under different promotion budgets is shown in Figure 5. From Figure 5(a), we observe

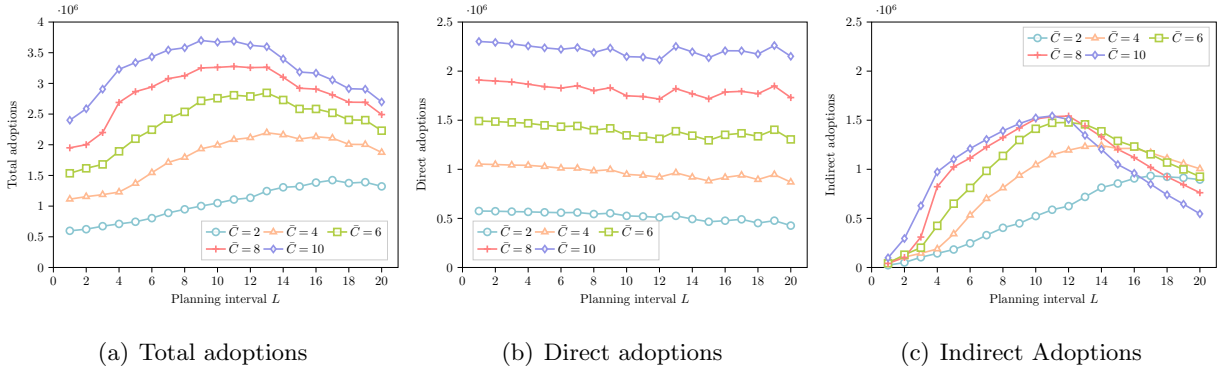|		
(a) Total adoptions	(b) Direct adoptions	(c) Indirect Adoptions

Figure 5   **Number of adoptions at $t = 120$ of the AGA policy with different selections of promotion budget.**

an initial increase followed by a decrease in total adoptions as L increases. As shown in 5(b),

direct adoptions exhibit a consistent decrease with an increase in L. This is expected because a longer planning interval reduces direct adoptions from promotion to potentially increase indirect adoptions driven by diffusion. Similar to the total adoptions, the indirect adoption curve assumes an inverted U-shape, a phenomenon driven by the fact that when L is too large, the algorithm suffers from infrequent updates, losing the diffusion power for new videos due to timeliness.

Furthermore, we investigate how the AGA policy with different L values distributes the promotion budget among videos based on their promotion and diffusion coefficients. Figure 6 shows the average promotion times received by videos in different categories. Although videos with a large p
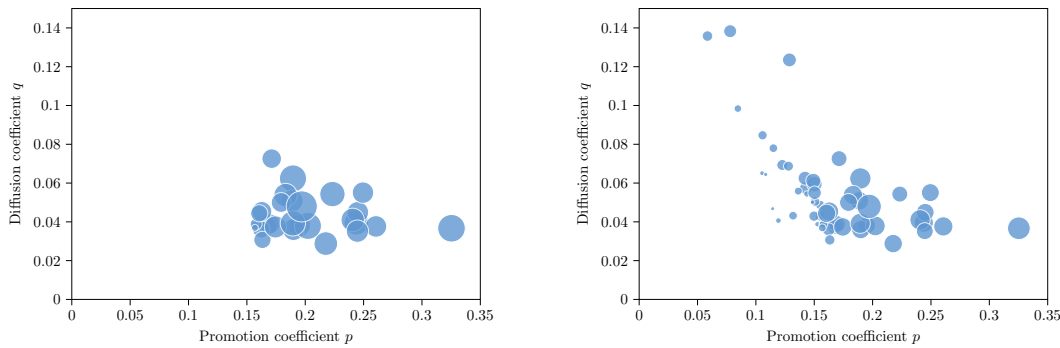

Figure 6   Illustration of the AGA policy across different video categories. Each point in the scatter plot represents a video category. The size of points represents the average promotion times of each category. **Left:** $L = 1$; **Right:** $L = 20$.

value tend to receive more promotion, clearly as L increases, the AGA policy increases the budget allocated to the videos with a large diffusion coefficient q to trigger more long-term diffusion. The judicious allocation of limited resources is governed by our algorithm.

6.3.2.   The underlying mechanism of the AGA policy. To gain deeper insights into the mechanism underlying the AGA policy and promote a qualitative understanding of how to manage the interactions of promotion and diffusion effects, we conduct additional analysis of the promotion fraction for videos, focusing on different model primitives. For illustration, we select $L = 13$, which consistently performs well across different promotion budgets in our experiments.

We aim to understand how a video's configuration (the promotion coefficient p_v and the diffusion coefficient q_v) and lifetime (cumulative adoption number $A_{v,t-1}$) affect the promotion fraction $x_{v,t}$ in the AGA policy. We use our experimental results as observations, where each observation represents a promotion fraction $x_{v,t}$ allocated to a video v at the beginning of time t. We divide the observations into six stages based on video lifetime. Stage 0 includes observations with $A_{v,t-1} = 0$, and stages $i \in \{1, 2, 3, 4, 5\}$ include observations when the video v has an adopter number $A_{v,t-1}$ at the start of time t such that $i = \lceil 5A_{v,t-1}/m \rceil$.

We first conduct a sensitivity analysis to examine how video configurations impact the promotion fraction x. This analysis uses linear regression to study the effects of p and q while controlling other relevant covariates. For a detailed explanation of this analysis, please refer to Section B.2.2. The regression coefficients of p and q, which we interpret as their impacts, are presented in Figure 7. Figure 7(a) demonstrates that both p and q positively influence x, most significantly at stage

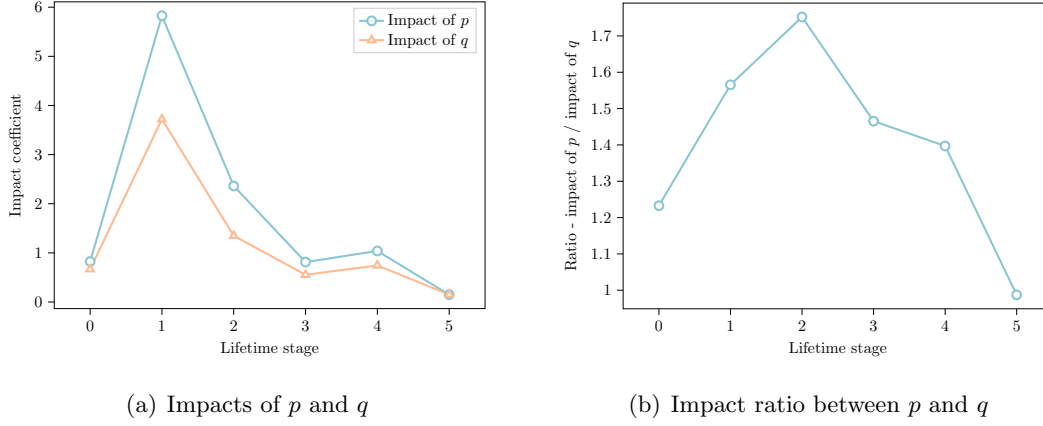(a) Impacts of p and q (b) Impact ratio between p and q

Figure 7   **The impacts of video configurations on the AGA policy across different lifetime stages.**

1. Contrary to the intuitive expectation that the impact of p and q should decrease gradually after the initial stage, our findings suggest otherwise. The impact of p and q is most pronounced during the intermediate stages (i.e., stages 1 and 2). This is because, in the initial stage, the policy aims to kickstart the diffusion processes for a large pool of videos; so that it does not heavily differentiate between video configurations. The marginal returns of promoting different videos are about the same. In the intermediate stages, however, the policy becomes more selective, filtering out noncompetitive videos and favoring videos with greater potential based on their configurations. Furthermore, Figure 7(b) shows the impact ratio between p and q, indicating that p carries more weight than q, particularly during the intermediate stages.

Then, we use K-Means clustering to group video configurations into four clusters based on their lifetime promotion policies. The clustering procedure is described in Section B.2.3. Figure 8(a) displays the clustering results according to video configuration, while Figure 8(b) showcases the "average" promotion policy for each cluster. Several observations can be made. Despite the clusters being based on promotion policy, they strongly correlate with video configurations. Cluster 0, located in the bottom left of Figure 8(a), is distinct due to its notably lower promotion at stage 0. These are the videos "discarded" by the AGA policy due to their low value. Roughly speaking, moving towards the right of Figure 8(a), videos receive more promotions. Echoing the insights from our earlier sensitivity analysis, we notice a trend where the points of peak promotion shift towards
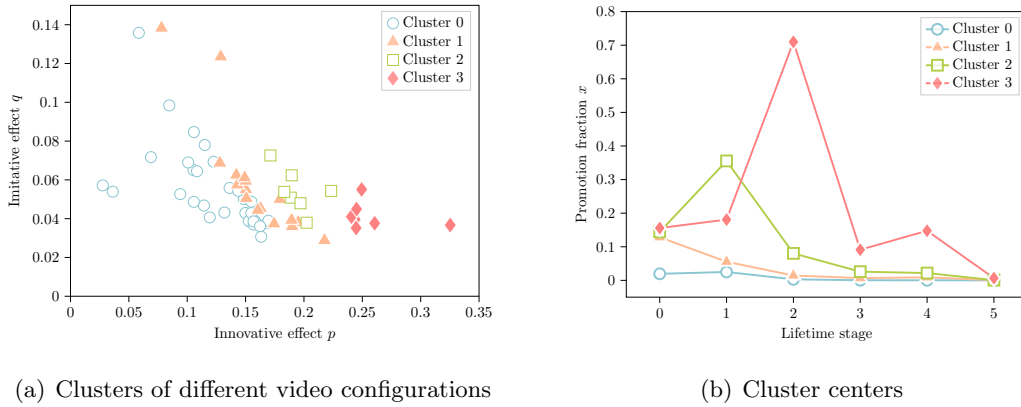
(a) Clusters of different video configurations   (b) Cluster centers

Figure 8   Illustration of the AGA policy clusters corresponding to different video configurations.

later stages in the videos' lifetime as p increases. In contrast, videos in Cluster 1 and 2 that have larger q values and smaller p values need to be promoted early to take advantage of their diffusion potential.

In summary, the AGA policy operates based on two main principles: (i) Promotion and diffusion effects, p and q, positively influence the promotion intensity, with the most profound impact during the intermediate lifetime stages. Among these, the promotion effect generally has a more notable impact. (ii) Videos with a small p but large q mainly receive their promotion in the early stages, where the promotion acts as a trigger for the diffusion process. In contrast, videos with a large p but small q continue to be promoted through early and intermediate stages, serving as both a trigger for diffusion and an attraction for direct adoptions. An interesting follow-up question is that if we can summarize these insights into heuristic policies that are easily implementable, in case complex optimization used in the AGA is not available. We present this discussion in Section B.2.4.

6.3.3.   Comparison with benchmarks. Finally, we compare the total adoptions of the AGA policy with benchmark policies, using the same experimental setting as in Section 6.3.1.

Benchmark policies: To ensure a fair comparison, we simulate the benchmark policies using the same diffusion process as our algorithm and compare the generated virtual rewards.

- *CGPO with accelerated greedy algorithm* (AGA). Our proposed algorithm as discussed in Section 4.3.2, with a planning horizon of $L = 13$.
- *CGPO without the diffusion effect* (NoD). This benchmark ignores the network effect. This is equivalent to the CGPO formulation when $L = 1$. It is a common practice in the industry that ignores the diffusion effects when promoting content.
- *Candidate Generation by Attractiveness* (ATT). This benchmark considers a heuristic CG strategy by selecting content that has the largest promotion potential $p_v(m - A_v)$. This benchmark speed up the CG procedure but overemphasizes the promotion effect.

- *Candidate Generation by Timeliness* (TIM). This benchmark considers a heuristic CG strategy by selecting content that is most recently added to the platform. This benchmark takes the timeliness of online content into account but overlooks the promotion effect.

- *Candidate Generation by Potential* (POT). This benchmark considers a heuristic CG strategy by selecting content that has the most number of new adopters at the previous time step. This benchmark illustrates the "rich-get-richer" principle.

Experiment result: Table 1 compares the performance of all benchmarks. We draw three key

Table 1   Total adoptions of different promotion policies

	NoD	AGA	ATT	TIM	POT
$\bar{C} = 2$	597,774	1,244,845	1,086,217	1,276,566	603,698
	-	108.25%	81.71%	113.44%	0.99%
$\bar{C} = 4$	1,113,254	2,195,978	1,984,325	2,127,953	916,924
	-	97.26%	78.25%	91.15%	-17.64%
$\bar{C} = 6$	1,534,981	2,846,019	2,691,889	2,664,396	1,048,988
	-	85.41%	75.37%	73.58%	-31.66%
$\bar{C} = 8$	1,950,074	3,262,392	3,172,585	3,081,788	1,202,599
	-	67.30%	62.69%	58.03%	-38.33%
$\bar{C} = 10$	2,400,101	3,597,649	3,534,973	3,401,598	1,265,783
	-	49.90%	47.28%	41.74%	-47.26%

Note: In each table cell, the first number represents the total adoptions under the benchmark, and the second number represents its relative improvement from NoD policy.

observations from the table. Firstly, AGA consistently performs well, ranking second only when $\bar{C} = 2$. The margin of AGA over other policies is remarkable. This indicates its robustness across different settings. Secondly, ATT and TIM also show notable improvement over NoD, suggesting the benefits of considering diffusion effects in promotion decisions. These benchmarks can be practical alternatives to AGA in real-world scenarios. Thirdly, POT performs even worse than NoD in most cases, indicating the potential drawbacks of the "rich-get-richer" principle. These observations highlight the importance of both candidate generation and diffusion effects for the content promotion problem and support the effectiveness of our proposed promotion policy.

Additional experiment results, including a heuristic-based promotion policy, a rolling horizon approach, and changing environment with increasing market size, are shown in Section B.2.4.

7.   Conclusion

In this study, we address the content promotion problem in online content platforms with the diffusion effect. We introduce a novel diffusion model to capture the platform's policy and the timeliness factor in online content diffusion. Based on this model, we formulate the candidate generation and promotion optimization (CGPO) problem. The problem is proved to be NP-hard,

and we offer an efficient approximation algorithm that exploits the problem structure. We also propose a double OLS method to estimate model parameters, leveraging the online platform data. Finally, we use a real-world dataset to validate the model, evaluate the performance, and provide managerial insights. Our empirical evidence underscores the importance of considering the diffusion effect in promotion optimization and supports the effectiveness of our proposed promotion policy.

There are several future directions for this study. First, we could investigate the impact of externalities between content pieces. For instance, similar content could potentially substitute each other, complicating the CGPO problem as the current submodularity results no longer apply. Second, we focus on an offline setting in this paper, where parameters are estimated beforehand. It can be quite interesting to consider the online version where parameters for new videos are estimated simultaneously with promotion optimization. The wealth of user and content information available on online platforms offers opportunities to explore this setting.

References

Agrawal, S., Yin, S., and Zeevi, A. (2021). Dynamic pricing and learning under the bass model. In Proceedings of the 22nd ACM Conference on Economics and Computation, pages 2–3.

AMZScout (2021). Amazon statistics for 2021 and the latest facts. https://amzscout.net/blog/amazon-statistics/.

Anandhan, A., Shuib, L., Ismail, M. A., and Mujtaba, G. (2018). Social media recommender systems: review and open research issues. IEEE Access, 6:15608–15628.

Bass, F. M. (1969). A new product growth for model consumer durables. Management science, 15(5):215–227.

Besbes, O., Gur, Y., and Zeevi, A. (2016). Optimization in online content recommendation services: Beyond click-through rates. Manufacturing & Service Operations Management, 18(1):15–33.

Chen, N. and Chen, Y.-J. (2021). Duopoly competition with network effects in discrete choice models. Operations Research, 69(2):545–559.

Chen, Y. and Shi, C. (2019). Joint pricing and inventory management with strategic customers. Operations Research, 67(6):1610–1627.

Covington, P., Adams, J., and Sargin, E. (2016). Deep neural networks for youtube recommendations. In Proceedings of the 10th ACM conference on recommender systems, pages 191–198.

Davidson, J., Liebald, B., Liu, J., Nandy, P., Van Vleet, T., Gargi, U., Gupta, S., He, Y., Lambert, M., Livingston, B., et al. (2010). The youtube video recommendation system. In Proceedings of the fourth ACM conference on Recommender systems, pages 293–296.

Du, C., Cooper, W. L., and Wang, Z. (2016). Optimal pricing for a multinomial logit choice model with network effects. Operations Research, 64(2):441–455.

Easingwood, C. J., Mahajan, V., and Muller, E. (1983). A nonuniform influence innovation diffusion model of new product acceptance. Marketing Science, 2(3):273–295.

Eckles, D., Esfandiari, H., Mossel, E., and Rahimian, M. A. (2022). Seeding with costly network information. Operations Research, 70(4):2318–2348.

Feng, J., Bhargava, H. K., and Pennock, D. M. (2007). Implementing sponsored search in web search engines: Computational evaluation of alternative mechanisms. INFORMS Journal on Computing, 19(1):137–148.

FOX32 (2020). Missing child alert canceled after 2 chipley girls found safe; mom in custody. `https://www.fox32chicago.com/news/missing-child-alert-canceled-after-2-chipley-girls-found-safe-mom-in-custody`.

Goldenberg, J., Libai, B., and Muller, E. (2001). Talk of the network: A complex systems look at the underlying process of word-of-mouth. Marketing letters, 12(3):211–223.

Golrezaei, N., Nazerzadeh, H., and Randhawa, R. (2020). Dynamic pricing for heterogeneous time-sensitive customers. Manufacturing & Service Operations Management, 22(3):562–581.

Graffius, S. M. (2022). Lifespan (life span) of social media posts. `https://www.scottgraffius.com/blog/files/tag-lifespan-0028half-life0029-of-social-media-posts003a-update-for-2022.html`.

Granovetter, M. (1978). Threshold models of collective behavior. American journal of sociology, 83(6):1420–1443.

Hu, M., Milner, J., and Wu, J. (2016). Liking and following and the newsvendor: Operations and marketing policies under social influence. Management Science, 62(3):867–879.

Jiang, Z. and Jain, D. C. (2012). A generalized norton–bass model for multigeneration diffusion. Management Science, 58(10):1887–1897.

Kempe, D., Kleinberg, J., and Tardos, É. (2003). Maximizing the spread of influence through a social network. In Proceedings of the ninth ACM SIGKDD international conference on Knowledge discovery and data mining, pages 137–146.

Kiesling, E., Günther, M., Stummer, C., and Wakolbinger, L. M. (2012). Agent-based simulation of innovation diffusion: a review. Central European Journal of Operations Research, 20(2):183–230.

Kitts, B., Freed, D., and Vrieze, M. (2000). Cross-sell: a fast promotion-tunable customer-item recommendation method based on conditionally independent probabilities. In Proceedings of the sixth ACM SIGKDD international conference on Knowledge discovery and data mining, pages 437–446.

Liu, J., Dolan, P., and Pedersen, E. R. (2010). Personalized news recommendation based on click behavior. In Proceedings of the 15th international conference on Intelligent user interfaces, pages 31–40.

Lu, W., Chen, S., Li, K., and Lakshmanan, L. V. (2014). Show me the money: dynamic recommendations for revenue maximization. Proceedings of the VLDB Endowment, 7(14):1785–1796.

Manshadi, V., Misra, S., and Rodilitz, S. (2020). Diffusion in random networks: Impact of degree distribution. Operations Research, 68(6):1722–1741.

Nemhauser, G. L., Wolsey, L. A., and Fisher, M. L. (1978). An analysis of approximations for maximizing submodular set functions—i. Mathematical programming, 14(1):265–294.

Norton, J. A. and Bass, F. M. (1987). A diffusion theory model of adoption and substitution for successive generations of high-technology products. Management science, 33(9):1069–1086.

Nosrat, F., Cooper, W. L., and Wang, Z. (2021). Pricing for a product with network effects and mixed logit demand. Naval Research Logistics (NRL), 68(2):159–182.

Schmittlein, D. C. and Mahajan, V. (1982). Maximum likelihood estimation for an innovation diffusion model of new product acceptance. Marketing science, 1(1):57–78.

Srinivasan, V. and Mason, C. H. (1986). Nonlinear least squares estimation of new product diffusion models. Marketing science, 5(2):169–178.

Statista (2021). Youtube average video length by category 2018. `https://www.statista.com/statistics/1026923/youtube-video-category-average-length/`.

Su, X. and Khoshgoftaar, T. M. (2009). A survey of collaborative filtering techniques. Advances in artificial intelligence, 2009.

Sultan, F., Farley, J. U., and Lehmann, D. R. (1990). A meta-analysis of applications of diffusion models. Journal of marketing research, 27(1):70–77.

Teng, J. T., Grover, V., and Guttler, W. (2002). Information technology innovations: general diffusion patterns and its relationships to innovation characteristics. IEEE transactions on engineering management, 49(1):13–27.

TikTok (2021). #squidgame hashtag videos on tiktok. `https://www.tiktok.com/tag/squidgame`.

Vahabi, H., Koutsopoulos, I., Gullo, F., and Halkidi, M. (2015). Difrec: A social-diffusion-aware recommender system. In Proceedings of the 24th ACM International on Conference on Information and Knowledge Management, pages 1481–1490.

Wang, R. and Wang, Z. (2017). Consumer choice models with endogenous network effects. Management Science, 63(11):3944–3960.

YouTube (2021). Youtube for press. `https://blog.youtube/press/`.

Zhang, H. and Vorobeychik, Y. (2019). Empirically grounded agent-based models of innovation diffusion: a critical review. Artificial Intelligence Review, pages 1–35.

Appendix A: Proofs and Supplements

A.1. Proofs and Supplements in Section 4

A.1.1. NP-hardness of the CGPO problem.

THEOREM 5 (**NP-Hardness**). *The CGPO problem (3) is NP-hard.*

Proof of Theorem 5: Consider a special instance of the CGPO problem when $L = 2$, $C = m$, $A_{v,0} = 0$ and $p_v \leq 1/2$ for all $v \in \mathcal{V}$. The conditions on p_v lead to the following two structures of the optimal solution:

(i) The constraint (4d) is achieved with equality at the optimal solution. Given the monotonicity of the adoptions regarding the promotion fraction, it is obvious that equality holds at the optimal solution since the promotion budget C is small, i.e., $C \leq m - A_{v,0} = m$ for any $v \in \mathcal{V}$.

(ii) $x_{v,2}^* = 0$ for all $v \in \mathcal{V}$. We show this by contradiction. Assume the optimal solution $x_{v,2}^* > 0$. We construct a feasible solution: $x_{v,1}' = x_{v,1}^* + x_{v,2}^*$ and $x_{v,2}' = 0$. Let $x_{v,1}^* + x_{v,2}^* = c_v \leq 1$. The optimal adoption is given by

$$A_{v,2}^* = -p_v^2 q_v m {x_{v,1}^*}^2 + p_v m q_v x_{v,1}^* + p_v m(x_{v,1}^* + x_{v,2}^*) = -p_v^2 q_v m {x_{v,1}^*}^2 + p_v m q_v x_{v,1}^* + p_v m c_v .$$

Similarly, the adoptions with $x_{v,1}'$ and $x_{v,2}'$ is $A_{v,2}' = -p_v^2 q_v m {x_{v,1}'}^2 + p_v m q_v x_{v,1}' + p_v m c_v$. Given $p_v \leq 1/2C$, we have $A_{v,2}' - A_{v,2}^* = p_v q_v m x_{v,2}^*(1 - p_v(x_{v,1}' + x_{v,1}^*)) \geq p_v q_v m x_{v,2}^*(1 - 2p_v) \geq 0$, contradicting with the assumption. Let $\alpha_v = p_v^2 q_v m$ and $\beta_v = p_v m(q_v + 1)$. The CGPO problem for this specific instance can be expressed as

$$\max_{\boldsymbol{x}, U \subseteq \mathcal{V}: |U| \leq K} \quad \sum_{v \in \mathcal{V}} -\alpha_v x_{v,1}^2 + \beta_v x_{v,1}$$

$$\text{s.t.} \quad \sum_{v \in \mathcal{V}} x_{v,1} \leq 1,$$

$$0 \leq x_{v,1} \leq \mathbb{1}\{v \in U\}, \forall v \in \mathcal{V}.$$

Consider s_v to be some arbitrary number such that $s_v \in [0, 1]$. We presume that for all $v \in \mathcal{V}$, $-2\alpha_v s_v + \beta_v = d_1$ and $\alpha_v s_v^2 = d_2$ where d_1 and d_2 are two given constants. Let $\ell(\boldsymbol{x}) = \sum_{v \in \mathcal{V}} -\alpha_v x_v^2 + \beta_v x_v$, we claim that

$$\ell(\boldsymbol{x}^*) \geq d_1 + d_2 K \iff \text{there exists } U \subseteq \mathcal{V} \text{ with } |U| = K \text{ and } \sum_{v \in U} s_v = 1 .$$

To prove this claim, we first express the objective value as

$$\ell(\boldsymbol{x}) = \sum_{v \in \mathcal{V}} -\alpha_v x_v^2 + \beta_v x_v \leq \sum_{v \in \mathcal{V}} \left[(-2\alpha_v s_v + \beta_v)(x_v - s_v) - a_v s_v^2 + \beta_v s_v \right] \cdot \mathbb{1}\{v \in U\}$$

$$= \sum_{v \in \mathcal{V}} (-2\alpha_v s_v + \beta_v) x_v + \alpha_v s_v^2 \cdot \mathbb{1}\{v \in U\} = \sum_{v \in \mathcal{V}} d_1 x_v + d_2 \cdot \mathbb{1}\{v \in U\} \leq d_1 + d_2 K .$$

where the first inequality follows from the concavity of $\ell(\cdot)$ and the final inequality follows since U contains at most K pieces. Equality holds if and only if $x_v = s_v$ for all $v \in U$ (i.e., $\sum_{v:v \in U} s_v = 1$). This claim allows us to reduce SUBSET-SUM to our problem as follows. Let the positive integers $b_1, \ldots b_n$, and B form an instance of SUBSET-SUM. Without loss of generality, we assume that $b_i \leq B$ for all $i \in \{1, 2, \ldots, n\}$. Let $s_i = b_i/B$. Therefore, there exists a subset $I \subseteq \{1, \ldots, n\}$ such that $\sum_{i \in I} s_i = 1$ if and only if the objective value $\ell(\boldsymbol{x}^*)$ is at least $d_1 + d_2 K$.

We then proceed by providing an example of the values of m, d_1, and d_2, which ensures that our construction serves as a valid CGPO instance. Let $\underline{s} = \min_{v \in \mathcal{V}} s_v$, $m = 64/\underline{s}^2$, $d_1 = m/2$ and $d_2 = 1$. Our construction assumes

$$\begin{cases} -p_v^2 q_v m s_v + p_v m(q_v + 1) &= d_1 \\ p_v^2 q_v m s_v^2 &= d_2 \end{cases}, \implies \begin{cases} p_v q_v + p_v &= \frac{1}{2} + \frac{2}{m s_v} \\ p_v q_v \cdot p_v &= \frac{1}{m s_v^2} \end{cases}.$$

Therefore, for any given s_v, we can solve p_v and q_v as demonstrated in Eqn. (15).

$$p_v = \frac{\frac{1}{2} + \frac{2}{m s_v} + \sqrt{\left(\frac{1}{2} + \frac{2}{m s_v}\right)^2 - \frac{4}{m s_v^2}}}{2} \text{ and } q_v = \frac{\frac{1}{2} + \frac{2}{m s_v} - \sqrt{\left(\frac{1}{2} + \frac{2}{m s_v}\right)^2 - \frac{4}{m s_v^2}}}{\frac{1}{2} + \frac{2}{m s_v} + \sqrt{\left(\frac{1}{2} + \frac{2}{m s_v}\right)^2 - \frac{4}{m s_v^2}}} . \tag{15}$$

To ensure that p_v and q_v provided in Eqn. (15) are valid within the context of P-BDM, we need further justifications. First, we need to ensure Eqn. (15) has real value solutions, that is,

$$\left(\frac{1}{2} + \frac{2}{ms_v}\right)^2 - \frac{4}{ms_v^2} = \frac{1}{4} + \frac{2}{ms_v} + \left(\frac{4}{m^2} - \frac{4}{m}\right)\frac{1}{s_v^2} \geq \frac{1}{4} + \frac{2}{m} + \left(\frac{4}{m^2} - \frac{4}{m}\right)\frac{1}{\underline{s}^2} = \frac{3}{16} + \frac{33}{16m} \geq 0.$$

Next, we need to validate that $p_v, q_v \geq 0$, $p_v \leq 1/2$, and $p_v + q_v \leq 1$. It is obvious that $p_v, q_v \geq 0$ by Eqn. (15). In order to show $p_v + q_v \leq 1$, it suffices to show that $p_v, q_v \leq 1/2$. To show $p_v \leq 1/2$, we have

$$\sqrt{\left(\frac{1}{2} + \frac{2}{ms_v}\right)^2 - \frac{4}{ms_v^2}} \leq \frac{1}{2} - \frac{2}{ms_v} \iff \frac{1}{2} - \frac{2}{ms_v} \geq 0 \text{ and } \sqrt{\left(\frac{1}{2} - \frac{2}{ms_v}\right)^2 + \frac{4}{ms_v} - \frac{4}{ms_v^2}} \leq \frac{1}{2} - \frac{2}{ms_v},$$

where the inequalities follow since $0 \leq s_v \leq 1$. To show $q_v \leq 1/2$, we have

$$\frac{1}{2} + \frac{2}{ms_v} \leq 3\sqrt{\left(\frac{1}{2} + \frac{2}{ms_v}\right)^2 - \frac{4}{ms_v^2}} \iff \left(\frac{1}{2} + \frac{2}{ms_v}\right)^2 - \frac{9}{2ms_v^2} \geq \frac{23}{128} + \frac{33}{16m} \geq 0.$$

In conclusion, we show that the CGPO problem is NP-hard by this specific instance. $\qquad\square$

A.1.2. Proofs for the PO-CR problem.

Proof of Theorem 1: To establish the equivalence of two problems, we need to show that for all optimal solutions of the PO-CR problem, equalities hold for all constraints (5). We will show this by contradiction.

Let $(\boldsymbol{x}^*, \boldsymbol{A}^*)$ and R^* be the optimal solution and optimal value of the PO-CR problem. Assume there exists $u \in U$ and $\tau \in \{1, \ldots, L\}$ such that the following inequality holds: $A_{u,\tau}^* < A_{u,\tau-1}^* + p_v m x_{u,\tau}^* + \frac{q_u}{m} A_{u,\tau-1}^*(m - A_{u,\tau-1}^*)$.

By the optimality of $(\boldsymbol{x}^*, \boldsymbol{A}^*)$, it is straightforward to confirm that $(\boldsymbol{x}_{U,\tau+1:L}^*, \boldsymbol{A}_{U,\tau+1:L}^*)$ is also the optimal solution of the following problem (16). Consequently, the optimal value of problem (16) is equal to R^*.

$$\max_{\boldsymbol{x} \geq \boldsymbol{0}, \boldsymbol{A}_{U,\tau+1:L}} \quad \sum_{v \in U} A_{v,L} \tag{16a}$$

$$\text{s.t.} \quad A_{v,\tau+1} \leq A_{v,\tau}^* + p_v m x_{v,\tau+1} + q_v \frac{A_{v,\tau}^*}{m}(m - A_{v,\tau}^*), \quad \forall v \in U, \tag{16b}$$

$$x_{v,\tau+1} \leq 1 - \frac{A_{v,\tau}^*}{m}, \quad \forall v \in U, \tag{16c}$$

$$A_{v,t} \leq A_{v,t-1} + p_v m x_{v,t} + q_v \frac{A_{v,t-1}}{m}(m - A_{v,t-1}), \forall v \in U \quad \forall t = \tau+2, \ldots, L, \tag{16d}$$

$$x_{v,t} \leq 1 - \frac{A_{v,t-1}}{m}, \quad \forall v \in U \quad \forall t = \tau+2, \ldots, L, \tag{16e}$$

$$m \sum_{t=\tau+1}^{L} \sum_{v \in U} x_{v,t} \leq C - m \sum_{t=1}^{\tau} \sum_{v \in U} x_{v,t}^*. \tag{16f}$$

We then construct a feasible solution $(\boldsymbol{x}', \boldsymbol{A}')$ for the PO-CR problem and let R' be the objective value:

(i) When $t = 1, 2, \ldots, \tau-1$, $\boldsymbol{x}_{U,t}' := \boldsymbol{x}_{U,t}^*$; When $t = 0, 1, \ldots, \tau-1$, $\boldsymbol{A}_{U,t}' := \boldsymbol{A}_{U,t}^*$.

(ii) When $t = \tau$, $\boldsymbol{x}_{U,t}' := \boldsymbol{x}_{U,t}^*$ and $A_{v,t}' := \begin{cases} A_{v,t-1}^* + p_v m x_{u,t-1}^* + q_v \frac{A_{v,t-1}^*}{m}(m - A_{v,t-1}^*), & \text{when } v \in \{u\}, \\ A_{v,t}^*, & \text{when } v \in U \setminus \{u\}. \end{cases}$

(iii) When $t = \tau+1, \ldots, L$, $(\boldsymbol{x}_{U,t}', \boldsymbol{A}_{U,t}')$ is defined as the optimal solution of the following problem (17):

$$\max_{\boldsymbol{x} \geq \boldsymbol{0}, \boldsymbol{A}_{U,\tau+1:L}} \quad (16a)$$

$$\text{s.t.} \quad A_{v,\tau+1} \leq A_{v,\tau}' + p_v m x_{v,\tau+1} + \frac{q_v}{m} A_{v,\tau}'(m - A_{v,\tau}'), \forall v \in U, \tag{17a}$$

$$x_{v,\tau+1} \leq 1 - \frac{A_{v,\tau}'}{m}, \quad \forall v \in U, \tag{17b}$$

$$(16d) - (16f).$$

As a consequence, the optimal value of problem (17) is also equal to R'.

In the following, we focus on problems (16) and (17). We aim to show that $R' > R^*$, which contradicts with the optimality of $(\boldsymbol{x}^*, \boldsymbol{A}^*)$. Firstly, to characterize the optimal solution for problem (16), we use Lagrangian multipliers

to introduce the constraints (16b), (16c) and (16f) into the objective function. Let Ω denote the feasible region constructed by constraints (16d), (16e). The dual problem can thus be expressed as

$$\min_{\boldsymbol{\lambda} \geq \mathbf{0}, \boldsymbol{\mu} \geq \mathbf{0}, \theta \geq 0} r(\boldsymbol{\lambda}, \boldsymbol{\mu}, \theta) + \sum_{v \in U} \lambda_v \left(A_{v,\tau}^* + \frac{q_v}{m} A_{v,\tau}^* (m - A_{v,\tau}^*) \right) + \sum_{v \in U} \mu_v \left(1 - \frac{A_{v,\tau}^*}{m} \right) + \theta C, \tag{18}$$

where $r(\boldsymbol{\lambda}, \boldsymbol{\mu}, \theta)$ is the optimal value function of a parameterized maximization problem as shown in (19):

$$r(\boldsymbol{\lambda}, \boldsymbol{\mu}, \theta) := \max_{\substack{\boldsymbol{x}_{U,\tau+1:L} \geq 0, \\ (\boldsymbol{x}, \boldsymbol{A})_{U,\tau+1:L} \in \Omega}} \sum_{v \in U} \left[A_{v,L} - \lambda_v A_{v,\tau+1} + (\lambda_v m p_v - \mu_v - \theta m) x_{v,\tau+1} - \theta m \left(\sum_{t=1}^{\tau} x_{v,t}^* + \sum_{t=\tau+2}^{L} x_{v,t} \right) \right]. \tag{19}$$

Notice that, in the maximization problem (19), variable $\boldsymbol{x}_{U,\tau+1}$ is not constrained by any other variables, but only by a constant 0. Thus, we can split problem (19) into two subproblems:

$$\max_{\substack{\boldsymbol{x}_{U,\tau+2:L} \geq 0, \\ (\boldsymbol{x}, \boldsymbol{A})_{U,\tau+1:L} \in \Omega}} \sum_{v \in U} \left[A_{v,L} - \lambda_v A_{v,\tau+1} - \theta m \left(\sum_{t=1}^{\tau} x_{v,t}^* + \sum_{t=\tau+2}^{L} x_{v,t} \right) \right] \quad \text{and} \quad \max_{\boldsymbol{x}_{U,\tau+1} \geq 0} \sum_{v \in U} (\lambda_v m p_v - \mu_v - \theta m) x_{v,\tau+1}.$$

We then optimize two subproblems separately. For the former subproblem, we denote its optimal value as $s(\boldsymbol{\lambda}, \theta)$. For the latter subproblem, the maximization problem can be further decomposed for each content piece $v \in U$ and we can easily derive the optimal solution and the value of function $r(\boldsymbol{\lambda}, \boldsymbol{\mu}, \theta)$ as follows:

$$x_{v,\tau+1}^* = \begin{cases} 0 & \text{when } \mu_v \geq m(\lambda_v p_v - \theta), \\ +\infty & \text{when } \mu_v < m(\lambda_v p_v - \theta), \end{cases} \quad \text{and} \quad r(\boldsymbol{\lambda}, \boldsymbol{\mu}, \theta) = \begin{cases} s(\boldsymbol{\lambda}, \theta) & \text{when } \theta > \min_{v \in U}(\lambda_v p_v - \frac{\mu_v}{m}), \\ +\infty & \text{o.w.} \end{cases}$$

We then substitute the value function of $r(\boldsymbol{\lambda}, \boldsymbol{\mu}, \theta)$ into the dual problem (18). To minimize the dual value, it is obvious that $r(\boldsymbol{\lambda}, \boldsymbol{\mu}, \theta)$ should not be infinity. Hence, the dual problem (18) can be reformulated as (20),

$$\min_{\boldsymbol{\lambda} \geq \mathbf{0}, \theta \geq 0} \left[s(\boldsymbol{\lambda}, \theta) + \sum_{v \in U} \lambda_v \left(A_{v,\tau}^* + \frac{q_v}{m} A_{v,\tau}^* (m - A_{v,\tau}^*) \right) + \theta C + \sum_{v \in U} \min_{\substack{\mu_v \geq 0, \\ \mu_v \geq m(\lambda_v p_v - \theta)}} \mu_v \left(1 - \frac{A_{v,\tau}^*}{m} \right) \right]. \tag{20}$$

The inner minimization of problem (20) can be represented as (21). For any $v \in U$,

$$\min_{\substack{\mu_v \geq 0, \\ \mu_v \geq m(\lambda_v p_v - \theta)}} \mu_v \left(1 - \frac{A_{v,\tau}^*}{m} \right). \tag{21}$$

Since $A_{v,\tau}^* \leq m$ always holds, when given the value of $(\boldsymbol{\lambda}, \theta)$, the optimal solution of μ_v should be $\mu_v^*(\boldsymbol{\lambda}, \theta) = \max\{0, m(\lambda_v p_v - \theta)\}$. Finally, we define the dual value function as

$$u(\boldsymbol{\lambda}, \theta; \boldsymbol{A}_{U,\tau}^*) := s(\boldsymbol{\lambda}, \theta) + \sum_{v \in U} \lambda_v \left(A_{v,\tau}^* + \frac{q_v}{m} A_{v,\tau}^* (m - A_{v,\tau}^*) \right) + \theta C + \sum_{v \in U} \left(1 - \frac{A_{v,\tau}^*}{m} \right) \max\{0, m(\lambda_v p_v - \theta)\}.$$

Similarly, for problem (17), we can also have the dual value function as

$$u(\boldsymbol{\lambda}, \theta; \boldsymbol{A}_{U,\tau}') := s(\boldsymbol{\lambda}, \theta) + \sum_{v \in U} \lambda_v \left(A_{v,\tau}' + \frac{q_v}{m} A_{v,\tau}' (m - A_{v,\tau}') \right) + \theta C + \sum_{v \in U} \left(1 - \frac{A_{v,\tau}'}{m} \right) \max\{0, m(\lambda_v p_v - \theta)\}.$$

Let $(\boldsymbol{\lambda}^*, \theta^*)$ and $(\boldsymbol{\lambda}', \theta')$ be the optimal dual variables for the dual problems of (16) and (17). Given that problems (16) and (17) are convex optimization problems, by invoking Slater's condition, strong duality holds for both problems. Thus, the optimal values for problems (16) and (17) can be represented as $R^* = u(\boldsymbol{\lambda}^*, \theta^*; \boldsymbol{A}_{U,\tau}^*)$ and $R' = u(\boldsymbol{\lambda}', \theta'; \boldsymbol{A}_{U,\tau}')$. Finally, we compare between R^* and R' and show that $R^* \leq R'$.

$$R^* - R' = u(\boldsymbol{\lambda}^*, \theta^*; \boldsymbol{A}_\tau^*) - u(\boldsymbol{\lambda}', \theta'; \boldsymbol{A}_\tau') \leq u(\boldsymbol{\lambda}', \theta'; \boldsymbol{A}_\tau^*) - u(\boldsymbol{\lambda}', \theta'; \boldsymbol{A}_\tau') \tag{22a}$$

$$= \sum_{v \in U} \lambda_v' \left(A_{v,\tau}^* + \frac{q_v}{m} A_{v,0}^* (m - A_{v,\tau}^*) \right) + \sum_{v \in U} \left(1 - \frac{A_{v,\tau}^*}{m} \right) \max\{0, m(\lambda_v' p_v - \theta')\}$$

$$- \left[\sum_{v \in U} \lambda_v' \left(A_{v,\tau}' + \frac{q_v}{m} A_{v,\tau}' (m - A_{v,\tau}') \right) + \sum_{v \in U} \left(1 - \frac{A_{v,\tau}'}{m} \right) \max\{0, m(\lambda_v' p_v - \theta')\} \right]$$

$$= \sum_{v \in U} \left[\lambda'_v \left((1+q_v)(A^*_{v,\tau} - A'_{v,\tau}) - \frac{q_v}{m}(A^{*}_{v,\tau}{}^2 - A'_{v,\tau}{}^2) \right) - \frac{1}{m} \max\{0, m(\lambda'_v p_v - \theta')\}(A^*_{v,\tau} - A'_{v,\tau}) \right]$$

$$= \sum_{v \in U} (A^*_{v,\tau} - A'_{v,\tau}) \left[\lambda'_v \left(1 + q_v - \frac{q_v}{m}(A^*_{v,\tau} + A'_{v,\tau}) \right) - \frac{1}{m} \max\{0, m(\lambda'_v p_v - \theta')\} \right]$$

$$\leq \sum_{v \in U} (A^*_{v,\tau} - A'_{v,\tau}) \left[\lambda'_v \left(1 + q_v - \frac{q_v}{m}(A^*_{v,\tau} + A'_{v,\tau}) \right) - \lambda'_v p_v \right] \tag{22b}$$

$$< \sum_{v \in U} (A^*_{v,\tau} - A'_{v,\tau}) \lambda'_v (1 - q_v - p_v) \tag{22c}$$

$$\leq 0, \tag{22d}$$

where (22a) follows since $(\boldsymbol{\lambda}^*, \theta^*)$ is the optimal solution to dual problem (18); (22b) follows due to the construction of $\boldsymbol{A}^*_\tau \leq \boldsymbol{A}'_\tau$ and the inherent non-negativity of dual variables (i.e., $\boldsymbol{\lambda}' \geq \boldsymbol{0}$ and $\theta' \geq 0$); (22c) follows since by definition $q_v \geq 0$, $A^*_{u,\tau} < A'_{u,\tau} \leq m$ and $A^*_{v,\tau} = A'_{u,\tau} \leq m$ for all $v \in U \setminus \{u\}$; (22d) follows from the definition $p_v + q_v \leq 1$.

As a result, $(\boldsymbol{x}', \boldsymbol{A}')$ is a feasible solution to the PO-CR problem while the resulting objective value R' is greater than R^*. This indicates that $(\boldsymbol{x}^*, \boldsymbol{A}^*)$ cannot be an optimal solution to the PO-CR problem.

In conclusion, the original PO problem (4) and the relaxed problem are equivalent. □

A.1.3.   Lemmas and proofs for the single-variable reformulation.   In the following, we include lemmas and proofs to validate the single-variable reformulation and to show that it remains a convex program.

LEMMA 3 (**Redundant Constraint**). *Constraint* (6c) *is redundant to the reformulation* (6).

Proof of Lemma 3:   Let $(\boldsymbol{x}^*, \boldsymbol{A}^*)$ be the optimal solution of the PO problem (4). By P-BDM dynamics (4b), we can deduce that the optimal adoption number $\boldsymbol{A}^*$ is non-decreasingly evolves over time (i.e., $A_{v,0} \leq A^*_{v,1} \leq \cdots \leq A^*_{v,L}$ for all $v \in U$). By Theorem 1, $(\boldsymbol{x}^*, \boldsymbol{A}^*)$ is also the optimal solution to the PO-CR problem. Therefore, for all $v \in U, t = 1, 2, \ldots, L$, constraint $x_{v,t} \leq 1 - A_{v,0}/m$ is redundant compared with $x_{v,t} \leq 1 - A_{v,t-1}/m$ in the PO-CR problem. □

Construction of Feasible Solution to Problem (7).

For any $v \in U$, given $\boldsymbol{x}_{v,:} \in [0, 1 - A_{v,0}/m]^L$, a feasible solution can be constructed by the following three steps:

Step 1: Set $t := 1$. Let $A_{v,1} := A_{v,0} + p_v m x_{v,1} + q_v A_{v,0}(m - A_{v,0})/m$. Then, increment t by 1, i.e., $t := t + 1$.

Step 2: Let $A_{v,t} = \min\{m(1 - x_{v,t+1}), A_{v,t-1} + p_v m x_{v,t} + q_v A_{v,t-1}(m - A_{v,t-1})/m\}$.

Step 3: Increment t by 1, i.e., $t := t + 1$. Repeat step 2, until $t = L + 1$. □

To demonstrate that single-variable reformulation (6) remains a convex program, it is sufficient to show that the objective is concave, given that all constraints are linear.

Proof of Lemma 1:   For simplicity, we omit the subscript v here. For any $\boldsymbol{x}^{(1)}$ and $\boldsymbol{x}^{(2)}$, let $\boldsymbol{x}^{(\lambda)} = \lambda \boldsymbol{x}^{(1)} + (1 - \lambda)\boldsymbol{x}^{(2)}$, and we want to show that $\lambda f(\boldsymbol{x}^{(1)}) + (1-\lambda)f(\boldsymbol{x}^{(2)}) \leq f(\boldsymbol{x}^{(\lambda)})$ holds for any $0 \leq \lambda \leq 1$.

Suppose $\boldsymbol{A}^{(1*)}$, $\boldsymbol{A}^{(2*)}$ and $\boldsymbol{A}^{(\lambda*)}$ are the optimal solutions to problem (7) with regard to $\boldsymbol{x}^{(1)}$, $\boldsymbol{x}^{(2)}$, and $\boldsymbol{x}^{(\lambda)}$, respectively. Let $\boldsymbol{A}^{(\lambda)} = \lambda \boldsymbol{A}^{(1*)} + (1 - \lambda)\boldsymbol{A}^{(2*)}$. We first show that $\boldsymbol{A}^{(\lambda)}$ is a feasible solution to problem (7) with regard to $\boldsymbol{x}^{(\lambda)}$ by verifying that it satisfies constraints (5) and (4c).

For constraint (5), we have

$$A^{(\lambda)}_{t-1} + pm x^{(\lambda)}_t + \frac{q}{m} A^{(\lambda)}_{t-1}(m - A^{(\lambda)}_{t-1}) - A^{(\lambda)}_t$$

$$= \lambda A^{(1*)}_{t-1} + (1-\lambda)A^{(2*)}_{t-1} + pm \left[\lambda x^{(1)} + (1-\lambda)x^{(2)} \right]$$

$$+ \frac{q}{m} \left[\lambda A^{(1*)}_{t-1} + (1-\lambda)A^{(2*)}_{t-1} \right] \left[m - \lambda A^{(1*)}_{t-1} - (1-\lambda)A^{(2*)}_{t-1} \right] - \left[\lambda A^{(1*)}_t + (1-\lambda)A^{(2*)}_t \right]$$

$$= \lambda \left[A^{(1*)}_{t-1} + pm x^{(1)}_{t-1} + q A^{(1*)}_{t-1} - A^{(1*)}_t \right] + (1-\lambda) \left[A^{(2*)}_{t-1} + pm x^{(2)}_{t-1} + q A^{(2*)}_{t-1} - A^{(2*)}_t \right] - \frac{q}{m} \left[\lambda A^{(1*)}_{t-1} + (1-\lambda)A^{(2*)}_{t-1} \right]^2$$

$$\geq \lambda \left[A^{(1*)}_{t-1} + pm x^{(1)}_{t-1} + q A^{(1*)}_{t-1} - A^{(1*)}_t \right] + (1-\lambda) \left[A^{(2*)}_{t-1} + pm x^{(2)}_{t-1} + q A^{(2*)}_{t-1} - A^{(2*)}_t \right]$$

$$- \frac{q}{m} \left[\lambda A_{t-1}^{(1*)2} + (1-\lambda) A_{t-1}^{(2*)2} \right] (\lambda + 1 - \lambda)$$

$$= \lambda \left[A_{t-1}^{(1*)} + pmx_{t-1}^{(1)} + \frac{q}{m} A_{t-1}^{(1*)} \left(m - A_{t-1}^{(1*)} \right) - A_t^{(1*)} \right] + (1-\lambda) \left[A_{t-1}^{(2*)} + pmx_{t-1}^{(2)} + \frac{q}{m} A_{t-1}^{(2*)} \left(m - A_{t-1}^{(2*)} \right) - A_t^{(2*)} \right]$$

$$\geq 0,$$

where the first inequality follows from Cauchy–Schwarz inequality, the second inequality follows since $\boldsymbol{A}^{(1*)}$ and $\boldsymbol{A}^{(2*)}$ satisfy the constraint (5) with regard to $\boldsymbol{x}^{(1)}$ and $\boldsymbol{x}^{(2)}$.

For constraint (4c), we have $1 - \frac{A_{t-1}^{(\lambda)}}{m} - x_t^{(\lambda)} = \lambda \left[1 - \frac{A_{t-1}^{(1*)}}{m} - x_t^{(1)} \right] + (1-\lambda) \left[1 - \frac{A_{t-1}^{(2*)}}{m} - x_t^{(2)} \right] \geq 0$, where the inequality follows since $\boldsymbol{A}^{(1*)}$ and $\boldsymbol{A}^{(2*)}$ satisfy the constraint (4c) with regard to $\boldsymbol{x}^{(1)}$ and $\boldsymbol{x}^{(2)}$.

Next, by the optimality of $\boldsymbol{A}^{(\lambda*)}$, we have $f(\boldsymbol{x}^{(\lambda)}) = A_L^{(\lambda*)} \geq A_L^{(\lambda)} = \lambda A_L^{(1*)} + (1-\lambda) A_L^{(2*)} = \lambda f(\boldsymbol{x}^{(1)}) + (1-\lambda) f(\boldsymbol{x}^{(2)})$. In conclusion, $f_v(\boldsymbol{x}_{v,:})$ is a concave function on the range $[0, 1 - A_{v,0}/m]^L$. $\square$

We then outline the optimality condition of the single-variable reformulation in Lemma 4. To facilitate the characterization of subgradient, we introduce the convex function $\tilde{f}_v := -f_v$. Let $\partial \tilde{f}_v(\boldsymbol{x}_v)$ be the subgradient set at $\boldsymbol{x}_v$:

LEMMA 4 **(Optimality Condition)**. *Given $\theta \geq 0$, the optimal solution $\boldsymbol{x}^*(\theta)$ to the inner maximization problem* (9) *satisfies the following condition.*

$$\forall v \in U, t = 1, 2, \ldots, L, \boldsymbol{g}_{v,:}(\theta) \in \partial \tilde{f}_v(\boldsymbol{x}_v^*(\theta)), \begin{cases} g_{v,t}(\theta) \geq -\theta & \text{when } x_{v,t}^*(\theta) = 0, \\ g_{v,t}(\theta) = -\theta & \text{when } 0 < x_{v,t}^*(\theta) < A_{v,0}, \\ g_{v,t}(\theta) \leq -\theta & \text{when } x_{v,t}^*(\theta) = A_{v,0}. \end{cases} \quad (23)$$

Proof of Lemma 4: Define $r_v(\boldsymbol{x}_{v,:}; \theta) := -\tilde{f}_v(\boldsymbol{x}_{v,:}) - \theta m \sum_{t=1}^L x_{v,t}$ for all $v \in U$. The problem is separable by content piece v, so we focus on a specific $v \in U$ in the following and omit the subscription for clarity.

When $x_t^*(\theta) = 0$, we construct a feasible solution $\boldsymbol{x}'(\theta) := \boldsymbol{x}^*(\theta) + \epsilon \boldsymbol{e}_t$ where ϵ is a sufficiently small positive constant and $\boldsymbol{e}_t$ is a vector with 1 in the t-th entry and 0 in all other entries. By the concavity of r, we have

$$r(\boldsymbol{x}'(\theta); \theta) \geq r(\boldsymbol{x}^*(\theta); \theta) - (\boldsymbol{g}(\theta) + \theta \mathbf{1})^\top (\boldsymbol{x}'(\theta) - \boldsymbol{x}^*(\theta)) = r(\boldsymbol{x}^*(\theta); \theta) - (g_t(\theta) + \theta) \epsilon,$$

where $\mathbf{1}$ is the all one vector. Given the optimality of $\boldsymbol{x}^*(\theta)$, $g_t(\theta) \geq -\theta$ should hold.

When $x_t^*(\theta) = A_{v,0}$, we construct a feasible solution $\boldsymbol{x}''(\theta) := \boldsymbol{x}^*(\theta) - \epsilon \boldsymbol{e}_t$. By concavity of r, we have

$$r(\boldsymbol{x}''(\theta); \theta) \geq r(\boldsymbol{x}^*(\theta); \theta) - (\boldsymbol{g}(\theta) + \theta \mathbf{1})^\top (\boldsymbol{x}''(\theta) - \boldsymbol{x}^*(\theta)) = r(\boldsymbol{x}^*(\theta); \theta) + (g_t(\theta) + \theta) \epsilon.$$

Given the optimality of $\boldsymbol{x}^*(\theta)$, $g_t(\theta) \leq -\theta$ should hold.

When $0 < x_t^*(\theta) < A_{v,0}$, we simultaneously construct two feasible solutions $\boldsymbol{x}'(\theta)$ and $\boldsymbol{x}''(\theta)$ as previous. Similarly, by optimality of $\boldsymbol{x}^*(\theta)$, $g_t(\theta) = -\theta$ should hold.

In conclusion, we can characterize this optimality condition based on the subgradient $\boldsymbol{g}(\theta)$ and θ. $\square$

For any $\theta \geq 0$, we denote $\left(\boldsymbol{x}_{v,:}^*(\theta) : v \in \mathcal{V}\right)$ as the optimal solution to (9), and let function $s(\theta; U) := m \sum_{v \in U} \sum_{t=1}^L x_{v,t}^*(\theta)$ describe the total optimal promotion times with dual variable θ. In the following, we establish the property of $s(\theta; U)$ for any given candidate set $U \subseteq \mathcal{V}$ in Lemma 5.

LEMMA 5 **(Monotonicity)**. *For any $U \subseteq \mathcal{V}$, $s(\theta; U)$ is a nonincreasing function in θ.*

Proof of Lemma 5: For all $\theta_1, \theta_2 \geq 0$, let $\boldsymbol{g}_v(\theta_1) \in \partial \tilde{f}_v(\boldsymbol{x}_{v,:}^*(\theta_1))$ and $\boldsymbol{g}_v(\theta_2) \in \partial \tilde{f}_v(\boldsymbol{x}_{v,:}^*(\theta_2))$ for all $v \in U$. By Lemma 4, for all $v \in U$, we have

$$\left(\boldsymbol{x}_{v,:}^*(\theta_1) - \boldsymbol{x}_{v,:}^*(\theta_2)\right)^\top \left(-\boldsymbol{g}_v(\theta_1) + \boldsymbol{g}_v(\theta_2)\right)$$

$$= \left(\boldsymbol{x}_{v,:}^*(\theta_1) - \boldsymbol{x}_v^*(\theta_2)\right)^\top (\theta_1 \cdot \mathbf{1} - \theta_2 \cdot \mathbf{1}) + \sum_{t=1}^L \left(x_{v,t}^*(\theta_1) - x_{v,t}^*(\theta_2)\right) \left(-\theta_1 - g_{v,t}(\theta_1)\right) + \sum_{t=1}^L \left(x_{v,t}^*(\theta_1) - x_{v,t}^*(\theta_2)\right) \left(\theta_2 + g_{v,t}(\theta_2)\right)$$

$$= (\theta_1 - \theta_2) \cdot \left(\boldsymbol{x}_{v,:}^*(\theta_1) - \boldsymbol{x}_{v,:}^*(\theta_2)\right)^\top \mathbf{1} + \sum_{t=1}^L \left(\mathbb{1}\{x_{v,t}^*(\theta_1) = 0\} + \mathbb{1}\{x_{v,t}^*(\theta_1) = A_{v,0}\}\right) \left(x_{v,t}^*(\theta_1) - x_{v,t}^*(\theta_2)\right) \left(-\theta_1 - g_{v,t}(\theta_1)\right)$$

$$+ \sum_{t=1}^L \left(\mathbb{1}\{x_{v,t}^*(\theta_2) = 0\} + \mathbb{1}\{x_{v,t}^*(\theta_2) = A_{v,0}\}\right) \left(x_{v,t}^*(\theta_1) - x_{v,t}^*(\theta_2)\right) \left(\theta_2 + g_{v,t}(\theta_2)\right).$$

We further discuss the latter two terms. We have

$$\begin{cases} x_{v,t}^*(\theta_1) - x_{v,t}^*(\theta_2) = -x_{v,t}^*(\theta_2) \leq 0, \text{ and } -\theta_1 - g_{v,t}(\theta_1) \leq 0, & \text{when } x_{v,t}^*(\theta_1) = 0, \\ x_{v,t}^*(\theta_1) - x_{v,t}^*(\theta_2) = A_{v,0} - x_{v,t}^*(\theta_2) \geq 0, \text{ and } -\theta_1 - g_{v,t}(\theta_1) \geq 0, & \text{when } x_{v,t}^*(\theta_1) = A_{v,0}; \end{cases}$$

$$\text{and } \begin{cases} x_{v,t}^*(\theta_1) - x_{v,t}^*(\theta_2) = x_{v,t}^*(\theta_1) \geq 0, \text{ and } \theta_2 + g_{v,t}(\theta_2) \geq 0, & \text{when } x_{v,t}^*(\theta_2) = 0, \\ x_{v,t}^*(\theta_1) - x_{v,t}^*(\theta_2) = x_{v,t}^*(\theta_2) - A_{v,0} \leq 0, \text{ and } \theta_2 + g_{v,t}(\theta_2) \leq 0, & \text{when } x_{v,t}^*(\theta_2) = A_{v,0}. \end{cases}$$

Given concavity of f_v, we have $0 \geq \left(\boldsymbol{x}_{v,:}^*(\theta_1) - \boldsymbol{x}_{v,:}^*(\theta_2)\right)^\top \left(-\boldsymbol{g}_v(\theta_1) + \boldsymbol{g}_v(\theta_2)\right) \geq (\theta_1 - \theta_2) \cdot \left(\boldsymbol{x}_{v,:}^*(\theta_1) - \boldsymbol{x}_{v,:}^*(\theta_2)\right)^\top \mathbf{1}$.
By summing up over $v \in U$, we have $(\theta_1 - \theta_2) \cdot m \sum_{v \in U} \sum_{t=1}^L \left[x_{v,t}^*(\theta_1) - x_{v,t}^*(\theta_2)\right] = (\theta_1 - \theta_2) \cdot (h(\theta_1) - h(\theta_2)) \leq 0$.
In conclusion, $s(\theta; U)$ is nonincreasing. $\quad\square$

Proof of Lemma 2: We begin by demonstrating that $s(\theta^*(U_2); U_1) \leq s(\theta^*(U_1); U_1)$. We can decompose the function $s(\theta; U_2)$ as $s(\theta; U_1) + s(\theta; U_2 \setminus U_1)$. We consider two cases based on the value of $s(\theta^*(U_1); U_1)$:

(i) $s(\theta^*(U_1); U_1) = C$. We directly have $s^*(\theta^*(U_2); U_1) \leq s^*(\theta^*(U_2); U_2) \leq C = s(\theta^*(U_1); U_1)$.

(ii) $s(\theta^*(U_1); U_1) < C$. We show this by contradiction. Assume that $s(\theta^*(U_2); U_1) > s(\theta^*(U_1); U_1)$. We can construct a feasible solution $\boldsymbol{x}'_{U_2,:}$ for the PO problem given candidate set U_2 as

$$\boldsymbol{x}'_{v,:} = \begin{cases} \boldsymbol{x}_{v,:}^*(\theta^*(U_1)) & \text{when } v \in U_1, \\ \boldsymbol{x}_{v,:}^*(\theta^*(U_2)) & \text{when } v \in U_2 \setminus U_1. \end{cases}$$

The objective value generated by $\boldsymbol{x}'_{U_2,:}$ is larger than $\boldsymbol{x}_{U_2,:}^*(\theta^*(U_2))$, given the optimality of $\boldsymbol{x}_{U_1,:}^*(\theta^*(U_1))$ for the PO problem with candidate set U_1. This contradicts with the optimality of $\boldsymbol{x}_{U_2,:}^*(\theta^*(U_2))$ for the PO problem with candidate set U_2.

Consequently, $s(\theta^*(U_2); U_1) \leq s(\theta^*(U_1); U_1)$. By Lemma 5, we conclude that $\theta^*(U_1) \leq \theta^*(U_2)$. $\quad\square$

A.1.4. Submodularity of the CGPO objective.

Proof of Theorem 2: It is easy to verify that $R(U; C) + R(\mathcal{V} \setminus U; 0)$ is a monotone function. By Eqn. (11), we have

$$R(U \cup \{w\}; C) + R(\mathcal{V} \setminus (U + \{w\}); 0) = \max_{0 \leq c \leq C} R(U; c) + R(\{w\}; C - c) + R(\mathcal{V} \setminus (U + \{w\}); 0)$$
$$\geq R(U; C) + R(\{w\}; 0) + R(\mathcal{V} \setminus (U + \{w\}); 0) = R(U; C) + R(\mathcal{V} \setminus U; 0).$$

Next, we focus on the proof of submodularity. To prove that $R(U; C) + R(\mathcal{V} \setminus U; 0)$ is a submodular function, we need to demonstrate that for any given $U_1 \subseteq U_2 \subseteq \mathcal{V}$ and $w \in \mathcal{V} \setminus U_2$, Eqn. (10) holds. Therefore, we compare the marginal gain of content piece w when given nested content sets U_1 and U_2 as follows:

$$R(U_1 \cup \{w\}; C) - R(U_1; C) - R(\{w\}; 0) - [R(U_2 + \{w\}; C) - R(U_2; C) - R(\{w\}; 0)]$$
$$= R(U_1; c^*(U_1)) + R(\{w\}; C - c^*(U_1)) - R(U_1; C) - R(\{w\}; 0)$$
$$\quad - [R(U_2; c^*(U_2)) + R(\{w\}; C - c^*(U_2)) - R(U_2; C) - R(\{w\}; 0)]$$
$$\geq R(U_1; c^*(U_2)) + R(\{w\}; C - c^*(U_2)) - R(U_1; C) - R(\{w\}; 0)$$
$$\quad - [R(U_2; c^*(U_2)) + R(\{w\}; C - c^*(U_2)) - R(U_2; C) - R(\{w\}; 0)]$$
$$= [R(U_1; c^*(U_2)) - R(U_1; C)] - [R(U_2; c^*(U_2)) - R(U_2; C)] = -\int_{z=c^*(U_2)}^C \theta^*(U_1; z)dz + \int_{z=c^*(U_2)}^C \theta^*(U_2; z)dz$$
$$= \int_{z=c^*(U_2)}^C [\theta^*(U_2; z) - \theta^*(U_1; z)] \, dz \geq 0.$$

where the first inequality follows since $c^*(U_1)$ is the optimal solution that maximizes problem (11) and the last inequality follows by Lemma 2.

In conclusion, $R(U; C) + R(\mathcal{V} \setminus U; 0)$ is a monotone submodular set function. $\quad\square$

A.2. Proofs and Supplements in Section 5

A.2.1. The OLS estimation method for the BDM.

According to Bass (1969), the OLS method of the BDM works as follows. Given a sequence of adoption data $\{(a_t, A_t)\}_{t=0}^T$, it assumes the following relationship: $a_t = \beta_1 + \beta_2 \cdot A_{t-1} + \beta_3 A_{t-1}^2 + \epsilon_t$, where $\beta_1 = pm$, $\beta_2 = q - p$ and $\beta_3 = -q/m$ are three different parameters to estimate; 1, A_{t-1}, and A_{t-1}^2 are considered as three observed covariates; ϵ_t is the independent white noise. For notation simplicity, we denote the covariate matrix and dependent variable as

$$Z = \begin{pmatrix} 1 & A_0 & A_0^2 \\ 1 & A_1 & A_1^2 \\ \vdots & \vdots & \vdots \\ 1 & A_{T-1} & A_{T-1}^2 \end{pmatrix} \text{ and } \boldsymbol{a} = \begin{pmatrix} a_1 \\ a_2 \\ \vdots \\ a_T \end{pmatrix}.$$

The OLS estimator $\hat{\boldsymbol{\beta}}$ can then be derived as $\hat{\boldsymbol{\beta}} = (Z^\top Z)^{-1} Z^\top \boldsymbol{a}$. Consequently, the estimators can be obtained as

$$\hat{m} = \frac{\hat{\beta}_2 \pm \sqrt{\hat{\beta}_2^2 - 4\hat{\beta}_1\hat{\beta}_2}}{2\hat{\beta}_3}, \ \hat{p} = \frac{\hat{\beta}_1}{\hat{m}}, \text{ and } \hat{q} = -\hat{\beta}_3\hat{m}.$$

However, these estimators suffer from large variances. In extreme cases (e.g., $\hat{m} = 0$), they even become invalid.

A.2.2. Proofs for the asymptotic analysis of the OLS-based estimators.

To streamline notation, we define the fixed-design covariate matrix for the n-th diffusion process as

$$Z_{(n)} = \begin{pmatrix} x_{1,(n)} & \bar{A}_{1,(n)}(1 - \bar{A}_{1,(n)}) \\ x_{2,(n)} & \bar{A}_{2,(n)}(1 - \bar{A}_{2,(n)}) \\ \vdots & \vdots \\ x_{n,(n)} & \bar{A}_{n,(n)}(1 - \bar{A}_{n,(n)}) \end{pmatrix}.$$

Proof of Theorem 3: We first consider the n-th D-OLS estimator for q, which is represented as

$$\hat{q}_{(n)}^{\text{D-OLS}} = q + \frac{\sum_{i=1}^n \left[A_{i,(n)}(1 - x_{i,(n)} - \frac{A_{i,(n)}}{m_{(n)}})\epsilon_{i,(n)}^{\text{i}} \right]}{\sum_{i=1}^n \left[A_{i,(n)}(1 - x_{i,(n)} - \frac{A_{i,(n)}}{m_{(n)}}) \right]^2} = q + \frac{\frac{1}{n}\sum_{i=1}^n \bar{A}_{i,(n)}(1 - x_{i,(n)} - \bar{A}_{i,(n)})\bar{\epsilon}_{i,(n)}^{\text{i}}}{\frac{1}{n}\sum_{i=1}^n \bar{A}_{i,(n)}^2(1 - x_{i,(n)} - \bar{A}_{i,(n)})^2}.$$

Let $\bar{\epsilon}^{\text{i}}$ denote the noise distribution with finite variance $\text{var}\left(\bar{\epsilon}^{\text{i}}\right) < \infty$, we can characterize the mean and variance of D-OLS estimator as follows:

$$\mathbb{E}\left[\hat{q}_{(n)}^{\text{D-OLS}}\right] = q + \frac{\frac{1}{n}\sum_{i=1}^n \bar{A}_{i,(n)}(1 - x_{i,(n)} - \bar{A}_{i,(n)}) \cdot \mathbb{E}\left[\bar{\epsilon}_{i,(n)}^{\text{i}}\right]}{\frac{1}{n}\sum_{i=1}^n \bar{A}_{i,(n)}^2(1 - x_{i,(n)} - \bar{A}_{i,(n)})^2} = q, \text{ and}$$

$$\text{var}\left(\hat{q}_{(n)}^{\text{D-OLS}}\right) = \frac{\frac{1}{n^2}\sum_{i=1}^n \bar{A}_{i,(n)}^2(1 - x_{i,(n)} - \bar{A}_{i,(n)})^2 \text{var}\left(\bar{\epsilon}_{i,(n)}^{\text{i}}\right)}{\left[\frac{1}{n}\sum_{i=1}^n \bar{A}_{i,(n)}^2(1 - x_{i,(n)} - \bar{A}_{i,(n)})^2\right]^2} = \frac{\tilde{Q}_{22,(n)}}{nQ_{22,(n)}^2} \text{var}\left(\bar{\epsilon}^{\text{i}}\right).$$

By Chebyshev's inequality, we have $\Pr\left(|\hat{q}_{(n)}^{\text{D-OLS}} - q| \geq k\right) \leq \frac{\tilde{Q}_{22,(n)}}{k^2 nQ_{22,(n)}^2} \text{var}\left(\bar{\epsilon}^{\text{i}}\right)$. Taking limits on both sides, we get

$$\lim_{n \to \infty} \Pr\left(|\hat{q}_{(n)}^{\text{D-OLS}} - q| \geq k\right) \leq \lim_{N \to \infty} \frac{1}{k^2} \frac{\tilde{Q}_{22,(n)} \text{var}\left(\bar{\epsilon}^{\text{i}}\right)}{nQ_{22,(n)}^2} = \frac{\text{var}\left(\bar{\epsilon}^{\text{i}}\right)}{k^2} \cdot \frac{\lim_{n \to \infty} \tilde{Q}_{22,(n)}}{\lim_{n \to \infty} Q_{22,(n)}^2} \cdot \lim_{n \to \infty} \frac{1}{n} = \frac{\tilde{Q}_{22} \text{var}\left(\bar{\epsilon}^{\text{i}}\right)}{k^2 Q_{22}^2} \cdot \lim_{n \to \infty} \frac{1}{n} = 0,$$

which implies that $\lim_{n \to \infty} \hat{q}_{(n)}^{\text{D-OLS}} = q$. Similarly, we consider the n-th D-OLS estimator for p, which is

$$\hat{p}_{(n)}^{\text{D-OLS}} = p + \frac{\sum_{i=1}^n \left[m_{(n)} x_{i,(n)} \left((q - \hat{q}_{(n)}^{\text{D-OLS}})x_{i,(n)} A_{i,(n)} + \bar{\epsilon}_{i,(n)}^{\text{d}}\right)\right]}{\sum_{t=1}^n (m_{(n)} x_{i,(n)})^2} = p + \frac{\frac{1}{n}\sum_{i=1}^n \left[x_{i,(n)} \left((q - \hat{q}_{(n)}^{\text{D-OLS}})x_{i,(n)} \bar{A}_{i,(n)} + \bar{\epsilon}_{i,(n)}^{\text{d}}\right)\right]}{\frac{1}{n}\sum_{i=1}^n x_{i,(n)}^2}.$$

We consider the following two terms separately:

$$\lim_{n \to \infty} \left(\frac{\frac{1}{n}\sum_{i=1}^n (q - \hat{q}_{(n)}^{\text{D-OLS}})x_{i,(n)}^2 \bar{A}_{i,(n)}}{\frac{1}{n}\sum_{t=1}^n x_{i,(n)}^2} \right) \text{ and } \lim_{n \to \infty} \left(\frac{\frac{1}{n}\sum_{i=1}^n x_{i,(n)} \bar{\epsilon}_{i,(n)}^{\text{d}}}{\frac{1}{n}\sum_{t=1}^n x_{i,(n)}^2} \right).$$

The first term converges to 0 since

$$\lim_{n \to \infty} \left(\frac{\frac{1}{n}\sum_{i=1}^n (q - \hat{q}^{\text{D-OLS}})x_{i,(n)}^2 \bar{A}_{i,(n)}}{\frac{1}{n}\sum_{t=1}^n x_{i,(n)}^2} \right) = \lim_{n \to \infty} \left(q - \hat{q}_{(n)}^{\text{D-OLS}} \right) \cdot \lim_{n \to \infty} \left(\frac{\tilde{Q}_{11,(n)}}{Q_{11,(n)}} \right) = \frac{\tilde{Q}_{11}}{Q_{11}} \lim_{n \to \infty} \left(q - \hat{q}_{(n)}^{\text{D-OLS}} \right) = 0.$$

The second term also converges to 0, similarly as in the proof of $\hat{q}_{(n)}^{\text{D-OLS}}$. As a result, we have $\lim_{n \to \infty} \hat{p}_{(n)}^{\text{D-OLS}} = p$.

In conclusion, D-OLS estimators $\hat{p}^{\text{D-OLS}}$ and $\hat{q}^{\text{D-OLS}}$ are consistent estimators. $\quad\square$

Proof of Theorem 4:   We consider two different estimation methods, respectively.

(i) The D-OLS method.

First, we characterize the limiting distribution of $\sqrt{n}(\hat{q}_{(n)}^{\text{D-OLS}} - q)$. We can represent it as

$$\sqrt{n}\left(\hat{q}_{(n)}^{\text{D-OLS}} - q\right) = \frac{\sqrt{n}\sum_{i=1}^{n}\left[\bar{A}_{i,(n)}(1 - x_{i,(n)} - \bar{A}_{i,(n)})\bar{\epsilon}_{i,(n)}^{\text{i}}\right]}{\sum_{i=1}^{n}\left[\bar{A}_{i,(n)}(1 - x_{i,(n)} - \bar{A}_{i,(n)})\right]^2} = \frac{\frac{1}{\sqrt{n}}\sum_{i=1}^{n}\left[\bar{A}_{i,(n)}(1 - x_{i,(n)} - \bar{A}_{i,(n)})\bar{\epsilon}_{i,(n)}^{\text{i}}\right]}{\frac{1}{n}\sum_{i=1}^{n}\bar{A}_{i,(n)}^2(1 - x_{i,(n)} - \bar{A}_{i,(n)})^2}.$$

We consider it as the sum of n independent random variables:

$$\sqrt{n}\left(\hat{q}_{(n)}^{\text{D-OLS}} - q\right) = \sum_{i=1}^{n} w_{i,(n)}\bar{\epsilon}_{i,(n)}^{\text{i}}, \text{ where } w_{i,(n)} = \frac{\frac{1}{\sqrt{n}}\left[\bar{A}_{i,(n)}(1 - x_{i,(n)} - \bar{A}_{i,(n)})\right]}{\frac{1}{n}\sum_{i=1}^{n}\bar{A}_{i,(n)}^2(1 - x_{i,(n)} - \bar{A}_{i,(n)})^2}.$$

We then show that this sequence satisfies

$$\lim_{n\to\infty}\max_{i=1,2,\dots,n}|w_{i,(n)}| \leq \lim_{n\to\infty}\frac{1}{\sqrt{n}}\cdot\frac{1}{\tilde{Q}_{22,(n)}} = \lim_{n\to\infty}\frac{1}{\sqrt{n}}\cdot\lim_{n\to\infty}\frac{1}{\tilde{Q}_{22,(n)}} = \lim_{n\to\infty}\frac{1}{\sqrt{n}}\cdot\frac{1}{\tilde{Q}_{22}} = 0.$$

where the inequality follows since $0 \leq x_{i,(n)}, \bar{A}_{i,(n)} \leq 1$ for all $i = 1, 2, \dots, n$.

This implies that Lindeberg's condition is satisfied. At last, the variance of $\sqrt{n}(\hat{q}_{(n)}^{\text{D-OLS}} - q)$ is as follows:

$$\text{var}\left(\sqrt{n}(\hat{q}_{(n)}^{\text{D-OLS}} - q)\right) = \frac{\frac{1}{n}\sum_{i=1}^{n}\bar{A}_{i,(n)}^2(1 - x_{i,(n)} - \bar{A}_{i,(n)})^2}{\left[\frac{1}{n}\sum_{i=1}^{n}\bar{A}_{i,(n)}^2(1 - x_{i,(n)} - \bar{A}_{i,(n)})^2\right]^2}\text{var}\left(\bar{\epsilon}_{i,(n)}^{\text{i}}\right) = \frac{1}{\tilde{Q}_{22,(n)}}\eta\sigma^2.$$

Let $\xi_2 = \eta Q_{22}/\tilde{Q}_{22} - 1$. By Lindeberg's central limit theorem, we have

$$\sqrt{n}(\hat{q}_{(n)}^{\text{D-OLS}} - q) \xrightarrow{d} \mathcal{N}\left(0, \frac{1}{Q_{22,(n)}}(1 + \xi_2)\sigma^2\right).$$

Next, we characterize the limiting distribution of $\sqrt{n}(\hat{p}_{(n)}^{\text{D-OLS}} - p)$. We can represent it as

$$\sqrt{n}(\hat{p}_{(n)}^{\text{D-OLS}} - p) = \frac{\sqrt{n}(q - \hat{q}_{(n)}^{\text{D-OLS}})\sum_{i=1}^{n}x_{i,(n)}^2\bar{A}_{i,(n)} + \sqrt{n}\sum_{i=1}^{n}x_{i,(n)}\bar{\epsilon}_{i,(n)}^{\text{d}}}{\sum_{i=1}^{n}x_{i,(n)}^2}$$

$$= \sqrt{n}(q - \hat{q}_{(n)}^{\text{D-OLS}})\frac{\frac{1}{n}\sum_{i=1}^{n}x_{i,(n)}^2\bar{A}_{i,(n)}}{\frac{1}{n}\sum_{i=1}^{n}x_{i,(n)}^2} + \frac{\frac{1}{\sqrt{n}}\sum_{i=1}^{n}x_{i,(n)}\bar{\epsilon}_{i,(n)}^{\text{d}}}{\frac{1}{n}\sum_{i=1}^{n}x_{i,(n)}^2}.$$

We consider the two terms separately. For the former term, we can easily derive that

$$\sqrt{n}(q - \hat{q}_{(n)}^{\text{D-OLS}})\frac{\frac{1}{n}\sum_{i=1}^{n}x_{i,(n)}^2\bar{A}_{i,(n)}}{\frac{1}{n}\sum_{i=1}^{n}x_{i,(n)}^2} \xrightarrow{d} \mathcal{N}\left(0, \frac{\eta\tilde{Q}_{11}^2}{\tilde{Q}_{22}Q_{11}^2}\sigma^2\right).$$

For the latter term, we perform a similar analysis as the previous one and get

$$\frac{\frac{1}{\sqrt{n}}\sum_{i=1}^{n}x_{i,(n)}\bar{\epsilon}_{i,(n)}^{\text{d}}}{\frac{1}{n}\sum_{i=1}^{n}x_{i,(n)}^2} \xrightarrow{d} \mathcal{N}\left(0, \frac{1-\eta}{Q_{11}}\sigma^2\right).$$

Let $\xi_1 = \eta(\tilde{Q}_{11}^2/\tilde{Q}_{22}Q_{11} - 1)$. As these two terms are independent, therefore, we can conclude that

$$\sqrt{n}(\hat{p}^{\text{D-OLS}} - p) \xrightarrow{d} \mathcal{N}\left(0, \frac{1}{Q_{11}}(1 + \xi_1)\sigma^2\right).$$

(ii) The OLS method. For notation simplicity, we write the OLS formulation in matrix form. Let $\boldsymbol{\beta} = (p, q)^{\top}$ and $\bar{\boldsymbol{\epsilon}}_{(n)} = (\bar{\epsilon}_{1,(n)}, \bar{\epsilon}_{2,(n)}, \dots, \bar{\epsilon}_{n,(n)})^{\top}$. Consider the limiting distribution of $\sqrt{n}(\hat{\boldsymbol{\beta}}_{(n)}^{\text{OLS}} - \boldsymbol{\beta})$, we have

$$\sqrt{n}(\hat{\boldsymbol{\beta}}_{(n)}^{\text{OLS}} - \beta) = \sqrt{n}\left(Z_{(n)}^{\top}Z_{(n)}\right)^{-1}Z_{(n)}^{\top}\bar{\boldsymbol{\epsilon}}_{(n)}.$$

Let $W_{(n)} = \sqrt{n}(Z_{(n)}^{\top}Z_{(n)})^{-1}Z_{(n)}^{\top}$ and $\boldsymbol{w}_{i,(n)}$ be the i-th column of $W_{(n)}$ for $i = 1, 2, \dots, n$. As a consequence, we can write $\sqrt{n}(\hat{\boldsymbol{\beta}}_{(n)}^{\text{OLS}} - \boldsymbol{\beta})$ as a sum of n independent random variables: $\sqrt{n}(\hat{\boldsymbol{\beta}}_{(n)}^{\text{OLS}} - \beta) = \sum_{i=1}^{n}\boldsymbol{w}_{i,(n)}\bar{\epsilon}_{i,(n)}$.

We then show that this sequence satisfies

$$\lim_{n\to\infty}\max_{i=1,2,\dots,n}\|\boldsymbol{w}_{i,(n)}\|_2 = \lim_{n\to\infty}\|W_{(n)}\|_{\infty,2} = \lim_{n\to\infty}\left\|\left(\frac{1}{n}Z_{(n)}^{\top}Z_{(n)}\right)^{-1}\frac{1}{\sqrt{n}}Z_{(n)}^{\top}\right\|_{\infty,2}$$

$$= \lim_{n\to\infty}\left\|Q_{(n)}^{-1}\frac{1}{\sqrt{n}}Z_{(n)}^{\top}\right\|_{\infty,2} \leq \lim_{n\to\infty}\frac{1}{\sqrt{n}}\left\|Q_{(n)}^{-1}\right\|_{2,\infty}\left\|Z_{(n)}^{\top}\right\|_{2,2}$$

$$\leq \lim_{n\to\infty}\frac{1}{\sqrt{n}}\left\|Q_{(n)}^{-1}\right\|_{2,\infty} = \lim_{n\to\infty}\frac{1}{\sqrt{n}}\cdot\lim_{n\to\infty}\left\|Q_{(n)}^{-1}\right\|_{2,\infty} = \lim_{n\to\infty}\frac{1}{\sqrt{n}}\cdot\left\|Q^{-1}\right\|_{2,\infty} = 0,$$

where the first inequality follows since the definition of matrix operator norm and the second inequality follows since $0 \le x_{i,(n)}, \bar{A}_{i,(n)} \le 1$ for all $i = 1, 2, \ldots, n$.

This implies that Lindeberg's condition is satisfied. Then, we calculate the variance of $\sqrt{n}(\hat{\boldsymbol{\beta}}^{\mathrm{OLS}} - \beta)$ as follows:

$$\mathrm{var}\left(\sqrt{n}(\hat{\boldsymbol{\beta}}_{(n)}^{\mathrm{OLS}} - \beta)\right) = \mathbb{E}\left[W_{(n)}\bar{\boldsymbol{\epsilon}}_{(n)}\bar{\boldsymbol{\epsilon}}_{(n)}^{\top}W_{(n)}^{\top}\right] = \sigma^2 W_{(n)}W_{(n)}^{\top} = n\left(Z_{(n)}^{\top}Z_{(n)}\right)^{-1} = Q_{(n)}^{-1}.$$

By Lindeberg's central limit theorem, we have

$$\sqrt{n}(\hat{\boldsymbol{\beta}}_{(n)}^{\mathrm{OLS}} - \boldsymbol{\beta}) \xrightarrow{d} \mathcal{N}\left(0, Q^{-1}\right), \text{ where } Q^{-1} = \begin{bmatrix} \frac{1}{Q_{11}}\left(1 + \frac{Q_{12}^2}{Q_{11}Q_{22}-Q_{12}^2}\right) & -\frac{Q_{12}}{Q_{11}Q_{22}-Q_{12}^2} \\ -\frac{Q_{12}}{Q_{11}Q_{22}-Q_{12}^2} & \frac{1}{Q_{22}}\left(1 + \frac{Q_{12}^2}{Q_{11}Q_{22}-Q_{12}^2}\right) \end{bmatrix}.$$

At last, we conclude that (i) The asymptotic variances of $\hat{p}^{\mathrm{D\text{-}OLS}}$ and $\hat{q}^{\mathrm{D\text{-}OLS}}$ are $(1+\xi_1)\sigma^2/Q_{11}$ and $(1+\xi_2)\sigma^2/Q_{22}$, where $\xi_1 = \eta(\tilde{Q}_{11}^2/\tilde{Q}_{22}Q_{11} - 1)$ and $\xi_2 = \eta Q_{22}/\tilde{Q}_{22} - 1$. (ii) The asymptotic variances of $\hat{p}^{\mathrm{OLS}}$ and $\hat{q}^{\mathrm{OLS}}$ are $(1+\kappa)\sigma^2/Q_{11}$ and $(1+\kappa)\sigma^2/Q_{22}$, where $\kappa = Q_{12}^2/|Q|$. $\square$

PROPOSITION 1. *When $\eta \le \tilde{Q}_{22}/Q_{22}$, we can show that the asymptotic variances of D-OLS estimators are smaller than those of OLS estimators, that is, $\xi_1 \le \kappa$ and $\xi_2 \le \kappa$.*

Proof for Proposition 1: Particularly, we have

$$\kappa - \xi_1 = \frac{Q_{12}^2}{Q_{11}Q_{22}-Q_{12}^2} - \eta\left(\frac{\tilde{Q}_{11}^2}{Q_{11}\tilde{Q}_{22}} - 1\right) \ge \frac{Q_{12}^2}{Q_{11}Q_{22}-Q_{12}^2} - \frac{\tilde{Q}_{11}^2}{Q_{11}\tilde{Q}_{22}} \ge \frac{Q_{12}^2 - \tilde{Q}_{11}^2}{Q_{11}Q_{22}} = \frac{Q_{12}+\tilde{Q}_{11}}{Q_{11}Q_{22}}\left(Q_{12} - \tilde{Q}_{11}\right)$$

$$= \frac{Q_{12}+\tilde{Q}_{11}}{Q_{11}Q_{22}}\lim_{n\to\infty}\left(\frac{1}{n}\sum_{i=1}^{n}x_{i,(n)}A_{i,(n)}(1-A_{i,(n)}) - \frac{1}{n}\sum_{i=1}^{n}x_{i,(n)}^2 A_{i,(n)}\right)$$

$$\ge \frac{Q_{12}+\tilde{Q}_{11}}{Q_{11}Q_{22}}\lim_{n\to\infty}\frac{1}{n}\sum_{i=1}^{n}\left(x_{i,(n)}A_{i,(n)} \cdot x_{i,(n)} - x_{i,(n)}^2 A_{i,(n)}\right) = 0.$$

where the first inequality follows since $0 \le \eta \le \tilde{Q}_{22}/Q_{22}$, the second inequality follows since $Q_{12}^2 \ge 0$ and the third inequality follows since $x_{i,(n)} \le 1 - \bar{A}_{i,(n)}$. Furthermore, we have

$$\kappa - \xi_2 = \frac{Q_{12}^2}{|Q|} - \left(\eta\frac{Q_{22}}{\tilde{Q}_{22}} - 1\right) \ge \kappa \ge 0.$$

where the first inequality follows since $\eta \le \tilde{Q}_{22}/Q_{22}$ and the second inequality follows by definition. $\square$

A.2.3. Proofs for the MLE estimators.

PROPOSITION 2. *When platforms cannot observe adopter types, the log-likelihood function $\mathcal{LL}^{MLE}(p,q)$ is concave.*

Proof of Proposition 2: To show that $\mathcal{LL}^{\mathrm{MLE}}(p,q)$ is concave, it is sufficient to show that the corresponding Hessian matrix is negative semi-definite.

Let $g_t = px_t/(1 - A_{t-1}/m) + qA_{t-1}/m$. The partial derivatives of $\mathcal{LL}^{\mathrm{MLE}}(p,q)$ with regard to p and q are

$$\frac{\partial\mathcal{LL}^{\mathrm{MLE}}(p,q)}{\partial p} = \sum_{t=1}^{T}\frac{\partial g_t}{\partial p}\left(\frac{a_t}{g_t} - \frac{m - A_{t-1} - a_t}{1 - g_t}\right) \text{ and } \frac{\partial\mathcal{LL}^{\mathrm{MLE}}(p,q)}{\partial q} = \sum_{t=1}^{T}\frac{\partial g_t}{\partial q}\left(\frac{a_t}{g_t} - \frac{m - A_{t-1} - a_t}{1 - g_t}\right).$$

Let $\boldsymbol{H}_{\mathcal{LL}}$ and $\boldsymbol{H}_{g_t}$ be the Hessian matrices of $\mathcal{LL}^{\mathrm{MLE}}$ and g_t, respectively. We have

$$\boldsymbol{H}_{\mathcal{LL}} = \sum_{t=1}^{T}\left[-\left(\frac{a_t}{g_t^2} + \frac{m - A_{t-1} - a_t}{(1 - g_t)^2}\right) \cdot \begin{pmatrix}\frac{\partial g_t}{\partial p} \\ \frac{\partial g_t}{\partial q}\end{pmatrix}\begin{pmatrix}\frac{\partial g_t}{\partial p} & \frac{\partial g_t}{\partial q}\end{pmatrix} + \left(\frac{a_t}{g_t} - \frac{m - A_{t-1} - a_t}{1 - g_t}\right) \cdot \boldsymbol{H}_{g_t}\right].$$

Since $\boldsymbol{H}_{g_t}$ is a zero matrix and $a_t/g_t^2 + (m - A_{t-1} - a_t)/(1 - g_t)^2 \ge 0$ always holds, we can conclude that $\boldsymbol{H}_{\mathcal{LL}}$ is negative semi-definite which implies $\mathcal{LL}^{\mathrm{MLE}}(p,q)$ is concave.

In conclusion, the log-likelihood function $\mathcal{LL}^{\mathrm{MLE}}(p,q)$ is concave. $\square$

PROPOSITION 3. *When platforms can observe adopter types, the log-likelihood function $\mathcal{LL}^{D\text{-}MLE}(p,q)$ is concave.*

Proof of Proposition 3: To show that $\mathcal{LL}^{\mathrm{D\text{-}MLE}}(p,q)$ is concave, it is sufficient to show that the corresponding Hessian matrix is negative semi-definite.

Let $g_t = qA_{t-1}/m$ and $h_t = p + qA_{t-1}/m$. The partial derivatives of $\mathcal{LL}^{\mathrm{D\text{-}MLE}}(p,q)$ with regard to p and q are

$$\frac{\partial \mathcal{LL}^{\mathrm{D\text{-}MLE}}(p,q)}{\partial p} = \sum_{t=1}^{T} \left[\frac{\partial g_t}{\partial p} \left(\frac{a_t^{\mathrm{i}}}{g_t} - \frac{m - A_{t-1} - mx_t - a_t^{\mathrm{i}}}{1 - g_t} \right) + \frac{\partial h_t}{\partial p} \left(\frac{a_t^{\mathrm{d}}}{h_t} - \frac{mx_t - a_t^{\mathrm{d}}}{1 - h_t} \right) \right], \text{ and}$$

$$\frac{\partial \mathcal{LL}^{\mathrm{D\text{-}MLE}}(p,q)}{\partial q} = \sum_{t=1}^{T} \left[\frac{\partial g_t}{\partial q} \left(\frac{a_t^{\mathrm{i}}}{g_t} - \frac{m - A_{t-1} - mx_t - a_t^{\mathrm{i}}}{1 - g_t} \right) + \frac{\partial h_t}{\partial q} \left(\frac{a_t^{\mathrm{d}}}{h_t} - \frac{mx_t - a_t^{\mathrm{d}}}{1 - h_t} \right) \right].$$

Let $\boldsymbol{H}_{\mathcal{LL}}$, $\boldsymbol{H}_{g_t}$ and $\boldsymbol{H}_{h_t}$ be the Hessian matrices of $\mathcal{LL}^{\mathrm{D\text{-}MLE}}$, g_t and h_t, respectively. We have

$$\boldsymbol{H}_{\mathcal{LL}} = \sum_{t=1}^{T} \left[-\left(\frac{a_t^{\mathrm{i}}}{g_t^2} + \frac{m - A_{t-1} - mx_t - a_t^{\mathrm{i}}}{(1 - g_t)^2} \right) \cdot \begin{pmatrix} \frac{\partial g_t}{\partial p} \\ \frac{\partial g_t}{\partial q} \end{pmatrix} \begin{pmatrix} \frac{\partial g_t}{\partial p} & \frac{\partial g_t}{\partial q} \end{pmatrix} + \left(\frac{a_t^{\mathrm{i}}}{g_t} - \frac{m - A_{t-1} - mx_t - a_t^{\mathrm{i}}}{1 - g_t} \right) \cdot \boldsymbol{H}_{g_t} \right]$$
$$+ \sum_{t=1}^{T} \left[-\left(\frac{a_t^{\mathrm{d}}}{h_t^2} + \frac{mx_t - a_t^{\mathrm{d}}}{(1 - h_t)^2} \right) \cdot \begin{pmatrix} \frac{\partial h_t}{\partial p} \\ \frac{\partial h_t}{\partial q} \end{pmatrix} \begin{pmatrix} \frac{\partial h_t}{\partial p} & \frac{\partial h_t}{\partial q} \end{pmatrix} + \left(\frac{a_t^{\mathrm{d}}}{g_t} - \frac{mx_t - a_t^{\mathrm{d}}}{1 - g_t} \right) \cdot \boldsymbol{H}_{h_t} \right].$$

Since $\boldsymbol{H}_{g_t}$ and $\boldsymbol{H}_{h_t}$ are zero matrices and $a_t^{\mathrm{i}}/g_t^2 + (m - A_{t-1} - mx_t - a_t^{\mathrm{i}})/(1 - g_t)^2 \geq 0$ and $a_t^{\mathrm{d}}/h_t^2 + (mx_t - a_t^{\mathrm{d}})/(1 - h_t)^2 \geq 0$ always hold, we can conclude that $\boldsymbol{H}_{\mathcal{LL}}$ is negative semi-definite which implies $\mathcal{LL}^{\mathrm{D\text{-}MLE}}(p,q)$ is concave.

In conclusion, the log-likelihood function $\mathcal{LL}^{\mathrm{D\text{-}MLE}}(p,q)$ is concave. $\square$

Appendix B: Supplements for Numerical Experiments

B.1. Model Calibration

B.1.1. Timeliness of online content diffusion. In this section, we will explore the concept of timeliness in online content and how it affects the diffusion process, resulting in a time-decay factor. We will begin by presenting our findings from data analysis and then modify the P-BDM to incorporate the time-decay factor for a better fit.

Online platforms operate in a highly dynamic and fast-paced environment, with new content being created and shared at a rapid rate. Compared to traditional markets, online platforms have a faster speed of information dissemination. As a result, the timeliness of online content plays a critical role. For example, a review video of a new movie will lose its relevance and generate fewer adoptions as the movie becomes older and less popular. Our analysis of the dataset from the video-sharing platform confirms this phenomenon. To demonstrate this, we calculate two ratios to characterize the promotion and diffusion effects:

$$\frac{a_{v,t}^{\mathrm{d}}}{mx_{v,t}} - \frac{a_{v,t}^{\mathrm{i}}}{m - A_{v,t-1}} \text{ and } \frac{a_{v,t}^{\mathrm{i}}}{\frac{A_{v,t-1}}{m}(m - A_{v,t-1})}. \tag{24}$$

We would like to remark that our goal with this analysis is not to calculate precise values of p and q, but rather to provide insight into the trends of both effects in the real world. As shown in Figure 9, the average values of these two ratios among all content pieces are presented against the time from $t = 1$ to $t = 50$. It is apparent from Figure 9 that the diffusion effect exhibits a time-decay trend, while the promotion effect remains nearly constant throughout the entire horizon. The sensitivity to timeliness is primarily observed in the diffusion effect. As such, incorporating the time-decay factor in diffusion modeling is critical to accurately capture the content adoptions for online platforms.

Recall that in the P-BDM dynamic (2), the diffusion effect is proportional to the cumulative adopter number, given by qA_{t-1}/m. To incorporate the timeliness of online content diffusion, we introduce a time-decay multiplicative factor γ where $0 < \gamma \leq 1$. Specifically, we consider the diffusion effect to be $q\gamma^{t-1}A_{t-1}/m$ instead. Therefore, the P-BDM with a time-decay factor can be shown as follows:

$$a_t = \underbrace{\left(p + q\frac{\gamma^{t-1}A_{t-1}}{m} \right) mx_t}_{\text{Direct adopters}} + \underbrace{q\frac{\gamma^{t-1}A_{t-1}}{m}(m - A_{t-1} - mx_t)}_{\text{Indirect adopters}} = \underbrace{pmx_t}_{\text{Promotion effect}} + \underbrace{q\frac{\gamma^{t-1}A_{t-1}}{m}(m - A_{t-1})}_{\text{Diffusion effect}}. \tag{25}$$
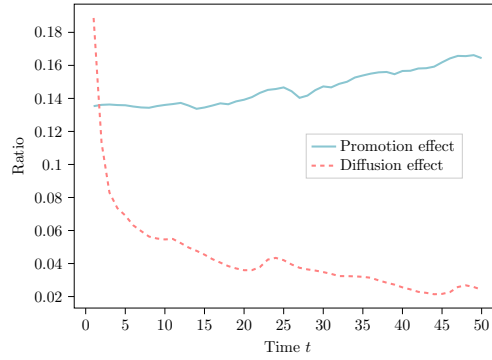
Figure 9 Illustration of the trends of promotion and diffusion effects. The x-axis represents the time elapsed since the video was uploaded to the platform and the y-axis represents the average values of the ratios as shown in Eqn. (24) among all videos at the same time step t.

This model uses the time-decay factor to characterize the decreasing incentive to diffuse the content as time elapses since its upload. When $\gamma = 1$, this model is equivalent to the original P-BDM.

We make two remarks here. First, the exponent of γ is related to the time elapsed since the content is uploaded. It should be distinguished from the subscript t in the CGPO problem, where the latter is used to denote the time since the beginning of the L planning period. Second, when γ is given, all the results in Sections 4 and 5 still hold. From the optimization perspective, it serves as a known parameter in the CGPO problem and does not change the underlying optimal structure. From the estimation perspective, it requires preprocessing of the observations, but the same estimation methods and analyses can be applied. Therefore, the P-BDM with a time-decay factor does not add to the difficulty of the entire problem but provides flexibility in characterizing the true adoption processes.

B.1.2. Group Estimation. In the context of online platforms, estimating parameters for each content piece individually is usually impractical because of the mountainous amount of videos and the scarcity of data pertaining to a video. What makes things worse is that we often have to make promotion decisions at the early stage of a video's life cycle with minimal data available for estimation. Consequently, it is reasonable to group or cluster the videos using features, and then estimate the parameters to make sure that past estimates can be generalized to future videos and the results are precise. Due to the lack of contextual information, we focus on using category labels for estimation.

The group estimation procedure is similar to that of a single piece, except that the observations are expanded to include all content pieces in the group. Let $\mathcal{V}^c \subseteq \mathcal{V}$ be the set of content pieces in the group c. Therefore, the observations for a group can be represented as $\cup_{v \in \mathcal{V}^c} \{(a_{v,t}^{\mathrm{d}}, a_{v,t}^{\mathrm{i}}, A_{v,t}, x_{v,t})\}_{t=1,2,\dots,T_v}$. The OLS-based and the MLE-based methods can be readily applied.

B.1.3. Calibration process. For each video category $c \in \mathcal{C}$ within the dataset, we split the observations into training, validation and test sets, separately. To avoid data corruption, we split the data based on video granularity, using a 60-20-20 split. Specifically, for the video set $\mathcal{V}^c \subseteq \mathcal{V}$ corresponding to category c, we randomly select 60% of the videos $v \in \mathcal{V}^c$ and assign the associated observations $\{(a_{v,t}^{\mathrm{d}}, a_{v,t}^{\mathrm{i}}, A_{v,t}, x_{v,t})\}_{t=1,2,\dots,T_v}$ to the training set. The remaining videos are also randomly split into 20% and 20% for validation and test sets, respectively.

To summarize the calibration process, we present Algorithm 2. We make a remark here, for each video $v \in \mathcal{V}$, we only include observations when the promotion fraction $x_{v,t}$ is positive in our training, validation, and test sets.

We evaluate the calibration performance using the weighted mean absolute percentage error (WMAPE). In Figure 10, we show the WMAPE we obtain by calibrating the P-BDM with different time-decay factor γ using the D-OLS method. The minimum WMAPE is achieved when $\gamma = 0.983$.

Algorithm 2: Calibration process with time-decay factor and group estimation.

---

1 **for** $c \in \mathcal{C}$ **do**
2   Randomly split the video set $\mathcal{V}^c$ into $\mathcal{V}^c_{\text{train}}$, $\mathcal{V}^c_{\text{valid}}$ and $\mathcal{V}^c_{\text{test}}$, using a 60-20-20 split.
3   Training set $\mathcal{D}_{\text{train}} := \cup_{v \in \mathcal{V}^c_{\text{train}}} \{(a^d_{v,t}, a^i_{v,t}, A_{v,t}, x_{v,t})\}_{t=1,2,\dots,T_v}$.
4   Valid set $\mathcal{D}_{\text{valid}} := \cup_{v \in \mathcal{V}^c_{\text{valid}}} \{(a^d_{v,t}, a^i_{v,t}, A_{v,t}, x_{v,t})\}_{t=1,2,\dots,T_v}$.
5   Test set $\mathcal{D}_{\text{test}} := \cup_{v \in \mathcal{V}^c_{\text{test}}} \{(a^d_{v,t}, a^i_{v,t}, A_{v,t}, x_{v,t})\}_{t=1,2,\dots,T_v}$.
6 **end**
7 **for** $\gamma \in \{\gamma_1, \gamma_2, \dots\}$ **do**
8   **for** $c \in \mathcal{C}$ **do**
9   Obtain $\hat{p}^c(\gamma)$ and $\hat{q}^c(\gamma)$ based on the training set $\mathcal{D}^{\text{train}}$ and time-decay factor γ.
10   **for** $v \in \mathcal{V}^c_{\text{valid}}$ **do**
11   Use $\hat{p}^c(\gamma)$ and $\hat{q}^c(\gamma)$ to predict adoptions as $\{\hat{a}_{v,t}\}_{t=1,2,\dots T_v}$.
12              $\text{WMAPE}_v(\gamma) := \sum_{t=1}^{T_v} |a_{v,t} - \hat{a}_{v,t}| / \sum_{t=1}^{T_v} a_{v,t} \times 100\%$.
13   **end**
14   **end**
15      $\text{WMAPE}(\gamma) := \frac{1}{|\mathcal{V}|} \sum_{v \in \mathcal{V}} \text{WMAPE}_v(\gamma)$.
16 **end**
17 $\gamma^* := \arg\max_\gamma \text{WMAPE}(\gamma)$.
18 **for** $c \in \mathcal{C}$ **do**
19   **for** $v \in \mathcal{V}^c_{\text{test}}$ **do**
20   Use $\hat{p}^c(\gamma^*)$ and $\hat{q}^c(\gamma^*)$ to predict adoptions as $\{\hat{a}_{v,t}\}_{t=1,2,\dots T_v}$.
21   **end**
22 **end**
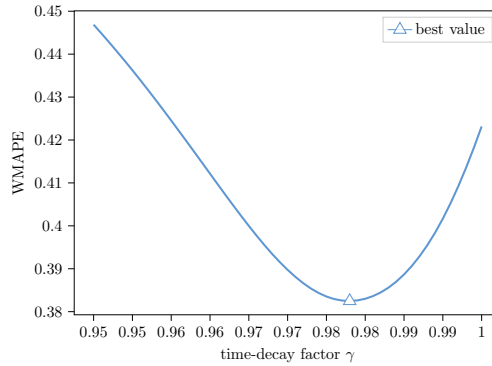
Figure 10   **WMAPE of the validation set against time-decay factor γ.**

For the sake of completeness, we also include the calibration results in Figure 11 when the timeliness is ignored (i.e., $\gamma = 1$). We observe that the estimated diffusion coefficient q is smaller in this case to account for the time decay in diffusion. However, the average out-of-sample WMAPE is 42.92%, which is 10% larger than when $\gamma = 0.983$. The average out-of-sample WMAPEs of the P-BDM with OLS and the BDM are 43.53% and 81.25%, respectively.

B.2.   Supplementary Analysis of the AGA Policy with $L = 13$

In this section, we provide a supplementary analysis of the AGA policy. We begin by examining the AGA policy across different lifetimes, followed by the detailed procedures of the sensitivity analysis and K-Means clustering analysis.
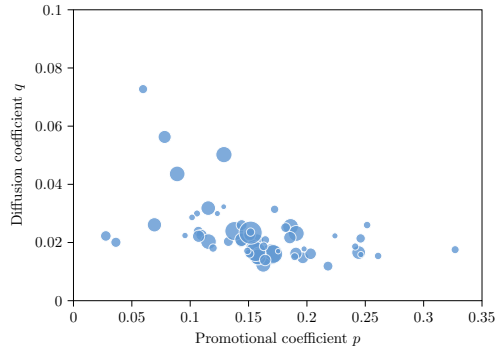
Figure 11   **Distribution of estimated coefficients when the timeliness of content diffusion is ignored** ($\gamma = 1$)**.**

B.2.1.   The AGA policy across different lifetime stages.   We begin by presenting the AGA policy across different lifetime stages in Figure 12. As shown in Figure 12(a), the policy primarily promotes videos in their initial
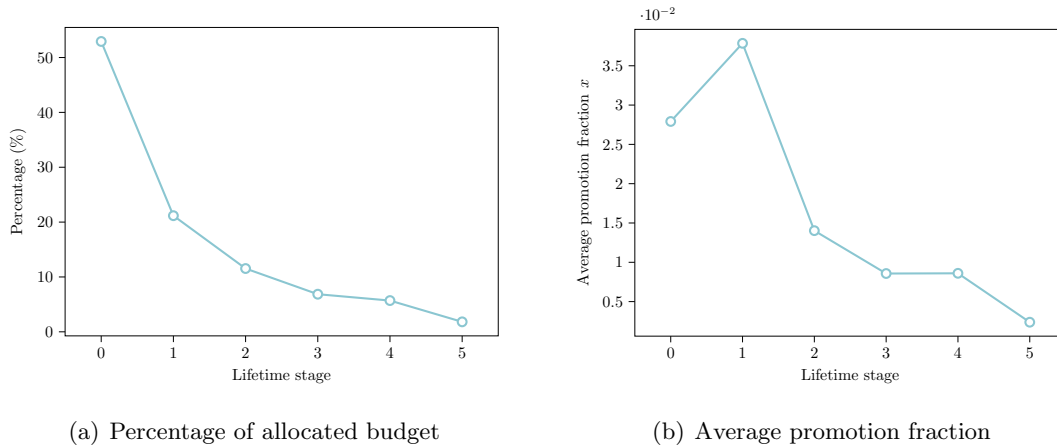

(a) Percentage of allocated budget

(b) Average promotion fraction

Figure 12   **Promotion budget allocation of the AGA policy for videos at different lifetime stages.**

stages, dedicating about 53% of the overall budget to videos that have no adopters (stage 0). This heavy initial promotion indicates the policy aims at sparking interest in new content. Figure 12(b) further emphasizes this point by showing that, on average, the promotion fraction allocated to videos tends to decline as the lifetime progresses. However, an exception can be observed at stage 1. This anomaly occurs because only a subset of videos is advanced to later stages after the initial promotion at stage 0. It implies that the policy also acts as a filter or selection mechanism, deciding if a video shows enough promise for further promotion. As a result, the policy generally allocates the promotion budget to videos that show considerable potential in their early stages.

B.2.2.   Sensitivity analysis of promotion and diffusion coefficients.   In order to understand the relationship between the promotion policy and the characteristics of videos, we perform sensitivity analysis for some important characteristics. For this purpose, we specify the following regression model for the allocated promotion fraction $x_{c,v,t}$, where each observation is a video v at the beginning of time t in the experiment with promotion budget $\bar{C} = c$:

$$x_{c,v,t} = \beta_0 + \beta_1 p_v + \beta_2 q_v + \beta_3 \bar{A}_{v,t-1} + \beta_4 c + \epsilon_{v,t}. \tag{26}$$

where the adoption number is normalized by the market size m before entering the regression. The coefficient $\boldsymbol{\beta}$ in Eqn. (26) can therefore be used to represent the impact of each characteristic on the allocated promotion fraction.

We conduct the regression on the observations from the previous AGA experiments with $L = 13$. Furthermore, in order to illustrate the difference of policy for videos at different lifetime, we perform regression within each lifetime stage separately. Table 2 reports the regression results. Although the R^2 is small for all the regressions, indicating

Table 2   Regression results of the promotion fraction of the AGA policy with regard to video characteristics

	# of Obs.	R^2	β_0 (const)	β_1 (p)	β_2 (q)	β_3 $(\bar{A})$	β_4 $(\bar{C})$
stage 0	72,867	0.044	-0.1412**** (0.0043)	0.8243**** (0.0216)	0.6687**** (0.0377)	- -	0.0055**** (0.0002)
stage 1	21,490	0.418	-1.1621**** (0.0245)	5.8253**** (0.1223)	3.7211**** (0.1035)	-0.7627**** (0.0195)	0.0576**** (0.0245)
stage 2	31,610	0.209	-0.4399**** (0.0145)	2.3614**** (0.0794)	1.3477**** (0.0527)	-0.1820**** (0.0101)	0.0121**** (0.0004)
stage 3	30,733	0.125	-0.2060**** (0.0079)	0.8130**** (0.0304)	0.5548**** (0.0248)	0.0563**** (0.0046)	0.0039**** (0.0002)
stage 4	25,460	0.213	-0.1825**** (0.0055)	1.0395**** (0.0298)	0.7441**** (0.0247)	-0.0714**** (0.0055)	0.0048**** (0.0002)
stage 5	29,340	0.085	0.0395**** (0.0021)	0.1499**** (0.0068)	0.1519**** (0.0080)	-0.0843**** (0.0039)	0.0003**** (0.0001)

Note: Robust standard errors are reported in parentheses. $^*p < 0.05$; $^{**}p < 0.01$; $^{***}p < 0.001$; $^{****}p < 0.0001$. For stage 0, $\bar{A}$ is not included in the regression since it takes 0 value for all observations.

that the linear regression model (26) is not a good representation of the complicated AGA policy, all coefficients are significant at the significance level of 0.0001. Therefore, we consider the values of regression coefficients can represent the impact of video characteristics on the promotion policy.

B.2.3. K-**Means clustering for the promotion policy.**   In order to further understand the AGA policy over the entire lifetime as a whole, we perform K-Means clustering on the average policy for different video configurations. Let $\mathcal{S} = \{0, 1, 2, 3, 4, 5\}$ be the set of lifetime stages. To summarize the clustering process, we present Algorithm 3.

Algorithm 3: K-Means clustering for the promotion policy of different video categories.

1 **for** $\underline{c \in \mathcal{C}}$ **do**
2   Classify observations $\cup_{v \in \mathcal{V}^c} \{A_{v,t-1}, x_{v,t}\}_{t=1,2,...,T}$ into different lifetime stages by $\bar{A}_{v,t-1}$.
3   **for** $\underline{s \in \mathcal{S}}$ **do**
4   Let $\mathcal{X}_s$ be the set of promotion fractions for observations at stage s.
5 $\tilde{x}_s^c := \sum_{x \in \mathcal{X}_s} x / |\mathcal{X}_s|$.
6   **end**
7 $\tilde{\boldsymbol{x}}^c := (\tilde{x}_s^c)_{s \in \mathcal{S}}^\top$. // `average promotion policy for category` c.
8 **end**
9 $\tilde{X} := (\tilde{\boldsymbol{x}}^c)_{c \in \mathcal{C}}$. // `feature matrix for all categories.`
10 Impute the missing values matrix $\tilde{X}$ using k-Nearest Neighbors, with $k = 2$.
11 Perform K-Means clustering based on $\tilde{X}$.

As shown in Algorithm 3, the clustering is solely based on the allocated promotion fraction generated by the AGA policy, and the promotion and diffusion coefficients are not explicitly involved. In Figure 13, we show the average promotion policies for different video categories by their clusters.
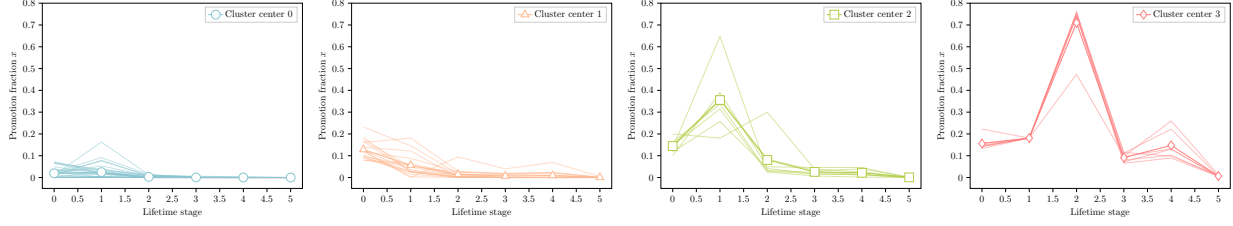
Figure 13   **Average promotion policies of different video categories (each subfigure represents a cluster).**

B.2.4. Additional experiments for performance evaluation.   Here, we present the additional experiment results. First, we propose a heuristic-based promotion policy and a rolling horizon approach and test their performance against benchmarks. Then, we test the AGA policy in a changing environment with increasing market size.

    Additional benchmark policies:

- *Heuristic-based promotion policy* (TREE). This benchmark is a heuristic promotion policy based on the experiment results of the AGA policy with $L = 13$. We train a decision tree to predict the promotion fraction that takes p, q, and the normalized adopter number $\bar{A}$ as input. To select the features at each split, we use mean squared error as the criterion for variance reduction. We set the minimum number of samples required to split an internal node to 50 to avoid overfitting. An illustrative representation of the top three levels of this decision tree, for the scenario of $\bar{C} = 6$, is given in Figure 14. The feature importance of p, q and $\bar{A}$ is 0.40, 0.07,
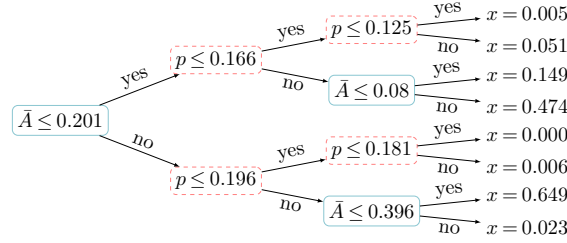

Figure 14   **Heuristic decision tree promotion policy rendered by the AGA policy for $\bar{C} = 6$ (top three levels).**

0.52, respectively. As shown in Figure 14, the splits at the top three levels are based on p and $\bar{A}$. However, it is important to note that the diffusion coefficient q still plays a crucial role. Although it is not prominently featured in the top-three-level splits, its effect can be reflected through the other two correlated features.

- *Rolling horizon approach* (RHA). This benchmark is a strategy we propose to address the limitation of the CGPO problem with larger planning intervals (L). As L increases, the CGPO solution can suffer from infrequent policy updates. RHA aims to mitigate this issue by continuously updating the promotion policy while compromising the future adoptions' description. To be specific, RHA solves the following PO subproblem (27) on a rolling horizon basis, rather than (4) when solving the CGPO problem:

$$\max_{\boldsymbol{x} \geq \boldsymbol{0}, \boldsymbol{A}_{1:L}} \quad (4\text{a})$$

$$\text{s.t.} \quad\quad\quad (4\text{b}) - (4\text{c}),$$

$$m \sum_{t=1}^{L} \sum_{v \in U} x_{v,t} \leq m\bar{C}, \quad\quad\quad\quad\quad\quad\quad (27\text{a})$$

$$x_{v,t} \leq 0, \quad\quad \forall v \in U \quad \forall t = 2, \ldots, L. \quad\quad\quad (27\text{b})$$

In the rolling horizon PO problem (27), the promotion fraction for the first period ($t = 1$) is determined while considering the total adoptions over the next L periods. The promotion fractions for subsequent periods ($t = 2, \ldots, L$) are assumed to be zero. Importantly, all results from Section 4 hold true for problem (27), implying that the AGA policy remains applicable for solving this problem, even in a rolling horizon context.

Additional experiment result: Table 3 compares the performance of the additional benchmarks. Table 3 shows

Table 3   **Total adoptions of additional promotion policies**

	NoD	AGA	TREE	RHA
$\bar{C} = 2$	597,774 -	1,244,845 108.25%	849,188 42.06%	1,035,649 73.25%
$\bar{C} = 4$	1,113,254 -	2,195,978 97.26%	1,418,229 27.39%	1,948,008 74.87%
$\bar{C} = 6$	1,534,981 -	2,846,019 85.41%	2,347,786 52.95%	2,661,580 73.39%
$\bar{C} = 8$	1,950,074 -	3,262,392 67.30%	2,799,755 43.57%	3,302,617 69.36%
$\bar{C} = 10$	2,400,101 -	3,597,649 49.90%	3,222,000 34.24%	3,815,859 58.99%

that both TREE and RHA significantly improve upon the NoD policy. Importantly, RHA outperforms AGA when the promotion budget is large. This suggests that with a sufficient promotion budget, infrequent updates to the promotion policy can lead to severe degradation. However, RHA demands solving the CGPO problem for each time period rather than L-period, potentially increasing computational load. In practice, the choice of the algorithm should consider factors like the platform's budget, the rate of new content upload, and computational capacity.

Increasing market size: To show the robustness of the AGA policy, we conduct experiments when the market size linearly increases with time. The results, presented in Table 4, follow the same experimental settings as in Section 6.3.1. We set the initial market size to $m = 10,000$, and with each new time step, 100 users join the platform. To address this increasing market size when solving the CGPO problem, we periodically update the market size every L periods. Table 4 shows similar results to Table 1, where the market size is assumed to be constant. This suggests

Table 4   **Total adoptions of different promotion policies with increasing market size**

	NoD	AGA	ATT	TIM	POT
$\bar{C} = 2$	1,007,830 -	2,062,601 104.66%	1,771,510 75.77%	2,138,443 112.18%	1,141,906 13.30%
$\bar{C} = 4$	1,943,360 -	3,549,797 82.66%	3,272,829 68.41%	3,602,208 85.36%	2,005,075 3.18%
$\bar{C} = 6$	2,708,316 -	4,724,322 74.44%	4,547,106 67.89%	4,612,666 70.31%	2,713,686 0.20%
$\bar{C} = 8$	3,584,133 -	5,586,073 55.86%	5,480,601 52.91%	5,426,749 51.41%	3,332,035 -7.03%
$\bar{C} = 10$	4,472,090 -	6,292,697 40.71%	6,201,900 38.68%	6,069,513 35.72%	3,741,837 -16.33%

that even though the periodic update approach may not fully capture the precise change in market size at each time step, it can effectively manage an increasing market size over the long term.